Icarus 220 (2012) 932–946

Contents lists available at SciVerse ScienceDirect

Icarus

journal homepage: www.elsevier.com/locate/icarus

Modeling ammonia–ammonium aqueous chemistries in the Solar System's icy bodies

G.M. Marion [a,*], J.S. Kargel [b], D.C. Catling [c], J.I. Lunine [d]

[a] Desert Research Institute, 2215 Raggio Parkway, Reno, NV 89512, USA
[b] Department of Hydrology & Water Resources, University of Arizona, Tucson, AZ 85721, USA
[c] Department of Earth & Space Sciences, University of Washington, Seattle, WA 98195, USA
[d] Cornell University, 402 Space Science Building, Ithaca, NY 14853, USA

ARTICLE INFO

Article history:
Received 8 June 2012
Accepted 11 June 2012
Available online 28 June 2012

Keywords:
Cosmochemistry
Geological processes
Mineralogy
Enceladus
Titan

ABSTRACT

The properties of ammonia and ammonium compounds in cold, subsurface brines are important for understanding the behavior of outer planet icy moons. The FREZCHEM model of aqueous chemistry was primarily designed for cold temperatures and high pressures, but does not contain ammonia and ammonium compounds. We added ammonia and ammonium compounds to FREZCHEM, and explored the role of these chemistries on Enceladus and Titan, mindful of their astrobiological implications. For the new FREZCHEM version, Pitzer parameters, volumetric parameters, and equilibrium constants for the Na–K–NH_4–Mg–Ca–Fe(II)–Fe(III)–Al–H–Cl–ClO_4–Br–SO_4–NO_3–OH–HCO_3–CO_3–CO_2–O_2–CH_4–NH_3–Si–H_2O system were developed for ammonia and ammonium compounds that cover the temperature range of 173–298 K and the pressure range of 1–1000 bars. Ammonia solubility was extended to 173 K, where $NH_3{\cdot}2H_2O$ and $NH_3{\cdot}H_2O$ precipitate, which is the lowest temperature in existing FREZCHEM versions. A subsurface "ocean" on Enceladus was simulated at 253 K with gas pressures, 1–10 bars, and with Na^+, Cl^-, HCO_3^-, $CO_2(g)$, $CH_4(g)$, and $NH_3(aq)$ that led to precipitation of ice, $NaHCO_3$, and gas hydrates ($CO_2{\cdot}6H_2O$ and $CH_4{\cdot}6H_2O$). The pH on Enceladus (Fig. 10) ranged from 5.74 to 6.76, and water activity, a_w, ranged from 0.80 to 0.82, which are relatively favorable for life. A subsurface "ocean" on Titan was simulated with NH_4^+, Cl^-, SO_4^{2-}, $CH_4(g)$, and $NH_3(aq)$ over the temperature range of 173–273 K that led to precipitation of $(NH_4)_2SO_4$, ice, $CH_4{\cdot}6H_2O$, and NH_4Cl. The CH_4 clathrate should float above the brine and is buoyant with respect to H_2O ice, so has the potential to be a source of CH_4 to replenish what has been photochemically destroyed in Titan's atmosphere over time. The pH in the Titan simulation (Fig. 11) ranged from 11.24 to 18.03 (latter may not be accurate), and a_w ranged from 0.28 to 0.72, which are relatively unfavorable for life as we know it. The Titan simulations, with total pressures of 10, 250, and 1000 bars, led to similar depositions, except for ice that failed to form under 1000 bars of pressure. In the past, there have been arguments for why Titan, given an early environment similar to Earth, could be a highly favorable body in our Solar System for life. But if Titan oceans are strongly alkaline with high pH whereas Enceladus' oceans have moderate pH, as simulated, the latter would seem a better environment for life as we know it. But bear in mind, caution must be exercised in quantifying the ammonia/ammonium cases because of the complexities and limitations of these chemistries in the FREZCHEM model.

1. Introduction

The completed *Galileo* mission to the Jupiter system and the continuing *Cassini–Huygens* mission to Saturn and its satellites, and the anticipation of the *New Horizons* flyby of the Pluto system and the *Dawn* mission that will orbit Ceres have stimulated considerable new thinking about the geochemical evolution of Europa, Enceladus, Titan, Pluto, outer main belt asteroids, and other icy bodies (Kargel et al., 2000; Baker et al., 2005; Cruikshank et al., 2005; Brown et al., 2006; Hussmann et al., 2006; Kieffer et al., 2006; Spencer et al., 2006; Waite et al., 2006, 2009, 2011; Yokano et al., 2006; Fortes, 2007, 2012; Fortes et al., 2007; Manga and Wang, 2007; Matson et al., 2007; Nimmo et al., 2007; Parkinson et al., 2007; Spencer and Grinspoon, 2007; Zolotov, 2007; Grindrod et al., 2008; Kieffer and Jakosky, 2008; Lorenz, 2008; Lorenz et al., 2008; McKinnon et al., 2008; Sotin and Tobie, 2008; Cooper et al., 2009; Postberg et al., 2009, 2011; Zolotov and Kargel, 2009; Sohl et al., 2010; Zolotov et al., 2011). Among the questions concerning the icy moons of the outer planets is the relevance of ammonia and ammonium compounds. These questions date back for decades

* Corresponding author. Fax: +1 775 673 7485.
E-mail address: Giles.Marion@dri.edu (G.M. Marion).

0019-1035/$ - see front matter © 2012 Elsevier Inc. All rights reserved.
http://dx.doi.org/10.1016/j.icarus.2012.06.016

and remain incompletely answered by observation (Lewis, 1972; Croft et al., 1988; Kargel et al., 1991; Kargel, 1992, 1998; Hogenboom et al., 1997; Brown and Calvin, 2000; Young, 2000; Leliwa-Kopystynski et al., 2002; Mousis et al., 2002). Whereas ammonia is widely considered, theoretically, to be broadly distributed and abundant in the outer Solar System, nondetections are the rule; definitive or probable observations of extraterrestrial ammonia and/or ammonium ion in our Solar System are rarer; these substances occur in the atmospheres of the gas giant planets, the plumes of Enceladus (Waite et al., 2009, 2011; Pizzarello et al., 2011; Zolotov et al., 2011), on large Kuiper Belt Objects such as Quaoar (Jewitt and Luu, 2004) and Orcus, and on Pluto's largest moon, Charon (Cook et al., 2007). Intense theoretical interest remains in possible ammonia–water volcanism on Titan and other icy satellites. Interest in possible sequestration of ammonia in ammonium solids and reactive destruction of ammonia (Kargel, 1992) has renewed timeliness to help explain why ammonia is rarely observed despite decades of searching for it. Recent investigations on the nature of internal fluids on icy moons has been stimulated by the *Cassini–Huygens* Mission (Baker et al., 2005; Tobie et al., 2005; Hussmann et al., 2006; Waite et al., 2006; Fortes et al., 2007; Spencer and Grinspoon, 2007; Smythe et al., 2009; Waite et al., 2009, 2011; Zolotov et al., 2011) and is pertinent to the upcoming Pluto/Charon/Kuiper Belt mission of *New Horizons*. On Earth, aqueous ammonia and ammonium salts are important in biology; the chemistries dealt with in this work may also have astrobiological consequences, which we briefly explore.

Ammonia and ammonium have not been found in the Solar System with the high abundances predicted theoretically, but after decades of fruitless searching, in the past decade especially, both ammonia and ammonium have been turning up in meteorite analyses and reflectance spectroscopic studies. Many comets emit 0.1–0.3% NH_3 and 3–10% CO_2 relative to H_2O. Carbonaceous chondrites generally contain ammonium at levels a few ppm to several tens of ppm. Direct detection of ammonia released by chemical treatment of the CM2 Murchison carbonaceous chondrite meteorite was thought to be due largely to release from ammonium salts as well as amines, amino acids and other compounds (Pizzarello et al., 1994); total NH_4^+ is ~20 ppm by mass. These compounds in carbonaceous chondrites all probably trace their origins to ammonia-based chemistry, including Strecker-type organic synthesis of ammonium cyanide from ammonia and hydrogen cyanide (Callahan et al., 2011), both comet-type volatiles. CR chondrites also are known to contain a similar suite of ammonia-related compounds, and additionally free ammonia was extracted (Pizzarello et al., 2011), though we suspect this may have been a break-down equilibrium product of decomposition of ammonium salts, some of which have a high ammonia vapor pressure. However, as mentioned, these all probably trace an origin back to ammonia chemistry.

Ammonia and derivatives such as amino acids are usually considered in the context of extant life, but biogenesis and prebiotic chemistry also emphasizes the key roles of these materials (e.g., Santana et al., 2010). Ammonium ion can be produced abiotically from other nitrogen compounds using a meteoritic nickel-rich metal catalyst (Smirnov et al., 2008). Ammonium thiocyanate, other ammonium compounds, and amino acids can be produced by electric discharges in CO_2–NH_3-bearing gas mixtures representing a popular model of Earth's primordial atmosphere.

The FREZCHEM model was primarily designed for cold temperatures and high pressures (Marion and Kargel, 2008), but until now did not contain ammonia and ammonium compounds. The specific objectives of this study were to (1) add ammonia–ammonium compounds to FREZCHEM, and (2) explore the role of these chemistries on outer planet satellites, especially with respect to low temperatures, high pressures, and the possibility of astrobiology. We note that there is also potential relevance of ammonia chemistry, not explored here, to (1) aqueous chemistry on Mars and large icy Main Belt asteroids, and to the origins of (2) the nitrogen-rich atmospheres of Earth and Titan, and of the solid nitrogen cryospheres and tenuous atmospheres of Triton, Pluto and some large Kuiper Belt Objects, such as Eris. And finally, the purpose of this paper is not to construct structural or thermal models of outer Solar System bodies, but to quantify the phase equilibria that should occur under relevant conditions and for a range of plausible constituents.

2. Methods and materials

2.1. FREZCHEM model

FREZCHEM is an equilibrium chemical thermodynamic model parameterized for concentrated electrolyte solutions (to ionic strengths = 20 molal) using the Pitzer approach (Pitzer, 1991, 1995) for the temperature range from 173 to 298 K (CHEMCHAU version has temperature range from 273 to 373 K) and the pressure range from 1 to 1000 bars (Marion and Farren, 1999; Marion, 2001, 2002; Marion et al., 2003, 2005, 2006, 2008, 2009a, 2009b, 2010a, 2010b, 2011; Marion and Kargel, 2008). Pressure beyond 1 bar was first added in Marion et al. (2005). The new version of the model, which includes ammonia and ammonium compounds, is parameterized for the Na–K–NH_4–Mg–Ca–Fe(II)–Fe(III)–Al–H–Cl–ClO_4–Br–SO_4–NO_3–OH–HCO_3–CO_3–CO_2–O_2–CH_4–NH_3–Si–H_2O system and includes 108 solid phases including ice, 16 chloride minerals, 36 sulfate minerals, 16 carbonate minerals, five solid-phase acids, four nitrate minerals, seven perchlorates, six acid-salts, five iron oxide/hydroxides, four aluminum hydroxides, two silica minerals, two ammonia minerals, two gas hydrates, and two bromide sinks (see above references for these model parameters, especially Marion and Kargel, 2008).

2.2. Pitzer approach

In the Pitzer approach, the activity coefficients (γ) as a function of temperature at 1.01 bar pressure for cations (M), anions (X), and neutral aqueous species (N), such as CO_2(aq) or CH_4(aq), are given by

$$\ln(\gamma_M) = z_M^2 F + \sum m_a(2B_{Ma} + ZC_{Ma}) + \sum m_c(2\Phi_{MC} + \sum m_a \Psi_{Mca}) + \sum\sum m_a m_{a'} \Psi_{maa'} + z_M \sum\sum m_c m_a C_{ca} + 2\sum m_n \lambda_{nM} + \sum\sum m_n m_a \zeta_{nMa} \quad (1)$$

$$\ln(\gamma_X) = z_X^2 F + \sum m_c(2B_{cX} + ZC_{cX}) + \sum m_a(2\Phi_{Xa} + \sum m_c \Psi_{cXa}) + \sum\sum m_c m_{c'} \Psi_{maa'X} + |z_X| \sum\sum m_c m_a C_{ca} + 2\sum m_n \lambda_{nX} + \sum\sum m_n m_c \zeta_{ncX} \quad (2)$$

$$\ln(\gamma_N) = 2\sum m_a \lambda_{Na} + \sum\sum m_c m_a \zeta_{Nca} + 2\sum m_n \lambda_{Nn} \quad (3)$$

where B, C, Φ, Ψ, λ and ζ are Pitzer-equation interaction parameters, m_i is the molal concentration, and F and Z are equation functions. In these equations, the Pitzer interaction parameters and the F function are temperature dependent. The subscripts c, a, and n refer to cations, anions, and neutral species, respectively. The coefficients c' and a' refer to cations and anions, respectively, that differ from c and a. The activity of water (a_w) at 1.01 bar pressure is given by

$$a_w = \exp\left(\frac{-\phi \sum m_i}{55.50844}\right) \quad (4)$$

where ϕ is the osmotic coefficient, which is given by

$$(\phi-1)=\frac{2}{\sum m_i}\left\{\frac{-A_\phi I^{3/2}}{1+bI^{1/2}}+\sum\sum m_c m_a\left(B^\phi_{ca}+ZC_{ca}\right)+\sum\sum m_c m_{c'}\left(\Phi^\phi_{cc'}+\sum m_a\Psi_{cc'a}\right)+\sum\sum m_a m_{a'}\left(\Phi^\phi_{cca'}+\sum m_c\Psi_{caa'}\right)+\sum\sum m_n m_c\lambda_{nc}+\sum\sum m_n m_a\lambda_{na}+\sum\sum\sum m_n m_c m_a\zeta_{nca}+(1/2)\sum m_n^2\lambda_{nn}\right\} \quad (5)$$

The binary B parameters in Eqs. (1), (2), and (5), are functions of C^0_{ca}, B^1_{ca}, and B^2_{ca}; similarly, the C parameters in these equations are a function of B^ϕ_{ca}.

FREZCHEM specifies the density of solutions and pressure dependence of equilibrium constants (K), activity coefficients (γ), and the activity of water (a_w). An example is how density is calculated with the equation

$$\rho=\frac{1000+\sum m_i M_i}{\frac{1000}{\rho^0}+\sum m_i\overline{V}^0_i+V^{ex}_{mix}} \quad (6)$$

where m_i is the molal concentration, M_i is the molar mass, ρ^0 is the density of pure water at a given temperature and pressure, $\overline{V}^0_i$ is the partial molar volume at infinite dilution of solution species, and V^{ex}_{mix} is the excess volume of mixing given by

$$V^{ex}_{mix}=A_v\left(\frac{I}{b}\right)\ln(1+bI^{0.5})+2RT\times\sum\sum m_c m_a\left[B^V_{c,a}+\left(\sum m_c z_c\right)C^v_{c,a}\right] \quad (7)$$

where A_v is the volumetric Pitzer–Debye–Hückel parameter, I is the ionic strength, b is a constant (1.2 $kg^{0.5}$ $mol^{-0.5}$), and $B^v_{c,a}$ and $C^v_{c,a}$ are functions of $B^{(0)V}_{c,a}$, $B^{(1)V}_{c,a}$, $B^{(2)V}_{c,a}$, and $C^V_{c,a}$. See Marion et al. (2005), Marion and Kargel (2008), or Marion et al. (2008) for a complete description of pressure equations that also rely on the volumetric parameters in Eq. (7).

The temperature dependencies of Pitzer parameters (discussed above) and solubility products (discussed below) are defined by the equation

$$P=a_1+a_2T+a_3T^2+a_4T^3+a_5/T+a_6\ln(T) \quad (8)$$

where P is the Pitzer parameter or $\ln(K_{sp})$ and T is absolute temperature (K); exceptions to this equation are footnoted in tables.

3. Results

3.1. Pitzer parameterization and solubility products

In this section, we present tables and figures that contain new equations relevant to ammonia and ammonium compounds. See earlier papers cited in Section 2.1 that document the range of previously published chemistries. A substantial fraction of the data references for FREZCHEM will rely on Linke (1965), largely because these data sets include chemistries at subzero temperatures that are critical for FREZCHEM.

The Pitzer parameters for the NH_4–Cl interactions at 298.15 K were taken from Pitzer (1991). These parameters were extended to lower temperatures by fitting to NH_4Cl–ice data from Linke (1965) (Fig. 1) using the equation

$$P_T=P_{298.15}+A(298.15-T) \quad (9)$$

where P is the Pitzer parameter, T is temperature, and A is a derived constant. Knowing the freezing point depression of a solution in equilibrium with pure ice allows one to directly determine the activity of water (a_w) and the solution osmotic coefficient (ϕ, Eq. (4)), which then can serve as the thermodynamic foundation for estimating the value of Pitzer parameters (Eq. (5)). While Eq. (9) was used to estimate the temperature dependence, this equation was converted to our standard format (Eq. (8)) in Table 1. Parameterization of NH_4–Cl interaction parameters to 258 K (Fig. 1) allowed us to estimate the solubility product for NH_4Cl (Sal ammoniac) (Table 2) based on solubility data (Linke, 1965). The model-calculated eutectic for this system occurred at 257.65 K with NH_4Cl = 4.54 m, which is in good agreement with the literature values of 257.79 K with NH_4Cl = 4.58 m (Linke, 1965).

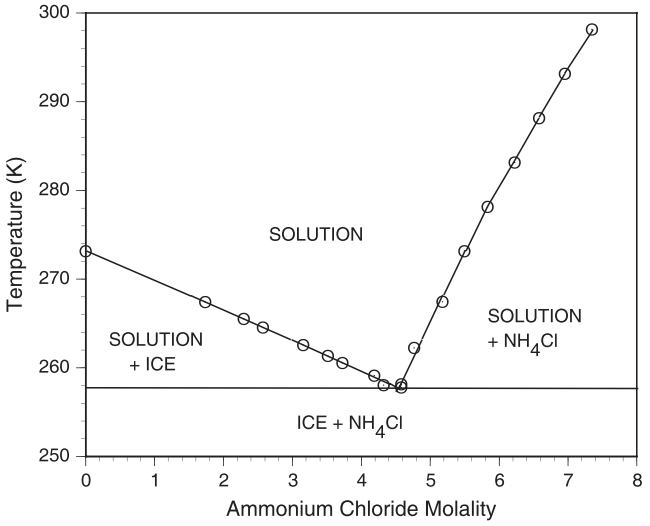

Fig. 1. Equilibrium of ammonium chloride in the 258–298 K temperature range. Symbols are experimental data; solid lines are model estimates.

The Pitzer parameters for NH_4–ClO_4 interactions at 298.15 K were taken from Pitzer (1991), and extended to lower temperatures with NH_4ClO_4–ice data from Linke (1965) (Fig. 2 and Table 1). In this particular case, there were only two ice data points (Fig. 2). Parameterization of the ice line to 270 K allowed us to estimate equilibrium constants for NH_4ClO_4 (Table 2). The solubility product of NH_4ClO_4 at the eutectic was model calculated at 270.41 K with NH_4ClO_4 = 0.93 m, which agrees with the literature values of 270.35 K at 0.93 m (Linke, 1965). NH_4ClO_4 is relatively insoluble compared to most perchlorate salts (e.g., Na, Mg, and Ca), except for $KClO_4$ that is also relatively insoluble (Marion et al., 2010a).

The Pitzer parameters for NH_4–NO_3 interactions at 298.15 K were taken from Pitzer (1991), and extended to lower temperatures by fitting NH_4NO_3–ice data from Linke (1965) (Fig. 3 and Table 1). The molality of NH_4NO_3 at 298 K is 26.8 m, which is beyond the upper limit for FREZCHEM (20 m). So we limited NH_4NO_3 to an upper concentration of 20 m, which is about 285 K (Fig. 3). Parameterization of the ice line to 256 K allowed us to estimate equilibrium constants for NH_4NO_3 (Table 2). The solubility product of NH_4NO_3 at the eutectic was model calculated as 256.35 K with NH_4NO_3 = 9.15 m, which are in excellent agreement with the literature values of 256.35 K with NH_4NO_3 = 9.20 m (Linke, 1965).

The Pitzer parameters for NH_4–HCO_3 interactions at 298.15 K were taken from Pitzer (1991), and extended to lower temperatures by fitting NH_4HCO_3–ice data from Linke (1965) (Fig. 4 and Table 1). In this particular case, there were only two ice data points (Fig. 4). Parameterization of the ice line to 269 K allowed us to estimate equilibrium constants for NH_4HCO_3 (teschemacherite) (Table 2). The solubility product of NH_4HCO_3 at the eutectic was model calculated at 269.05 K with NH_4HCO_3 = 1.32 m, which are in good agreement with the literature values of 269.25 K with NH_4HCO_3 = 1.33 m (Linke, 1965).

Table 1
Binary and volumetric Pitzer-equation parameters at 1.01325 bars derived in and this work or taken from the literature (numbers are in computer scientific notation where e ± xx stands for $10^{\pm xx}$).

	a_1	a_2	a_3	Temperature range (K)	Data sources
Pitzer-equation parameters					
$B^{(0)}_{NH_4,Cl}$	6.255e−2	−3.47e−5		258–303	Linke (1965), Pitzer (1991), and this work
$B^{(1)}_{NH_4,Cl}$	−1.992e0	7.323e−3		258–303	Linke (1965), Pitzer (1991), and this work
$C^{\phi}_{NH_4,Cl}$	−1.584e−2	4.302e−5		258–303	Linke (1965), Pitzer (1991), and this work
$B^{(0)}_{NH_4,ClO_4}$	−1.03e−2			270–307	Linke (1965), Pitzer (1991), and this work
$B^{(1)}_{NH_4,ClO_4}$	−2.610e0	8.69e−3		270–307	Linke (1965), Pitzer (1991), and this work
$C^{\phi}_{NH_4,ClO_4}$	0.0			270–307	Linke (1965), Pitzer (1991), and this work
$B^{(0)}_{NH_4,NO_3}$	−1.918e−1	5.916e−4		256–303	Linke (1965), Pitzer (1991), and this work
$B^{(1)}_{NH_4,NO_3}$	−1.132e0	4.171e−3		256–303	Linke (1965), Pitzer (1991), and this work
$C^{\phi}_{NH_4,NO_3}$	9.162e−3	−3.083e−5		256–303	Linke (1965), Pitzer (1991), and this work
$B^{(0)}_{NH_4,HCO_3}$	−3.80e−2			269–313	Linke (1965), Pitzer (1991), and this work
$B^{(1)}_{NH_4,HCO_3}$	9.257e−1	−2.87e−3		269–313	Linke (1965), Pitzer (1991), and this work
$C^{\phi}_{NH_4,HCO_3}$	0.0			269–313	Linke (1965), Pitzer (1991), and this work
$B^{(0)}_{NH_4,SO_4}$	−2.107e−1	8.378e−4		254–303	Linke (1965), Pitzer (1991), and this work
$B^{(1)}_{NH_4,SO_4}$	−6.089e0	2.265e−2		254–303	Linke (1965), Pitzer (1991), and this work
$C^{\phi}_{NH_4,SO_4}$	2.768e−2	−9.424e−5		254–303	Linke (1965), Pitzer (1991), and this work
Volumetric parameters					
$B^{v(0)}_{NH_4,Cl}$	4.687e−5	−1.307e−7		263–303	Linke (1965), Krumgalz et al. (1996), and this work
$B^{v(1)}_{NH_4,Cl}$	1.306e−3	−4.44e−6		263–303	Linke (1965), Krumgalz et al. (1996), and this work
$C^{v}_{NH_4,Cl}$	−8.623e−6	2.73e−8		263–303	Linke (1965), Krumgalz et al. (1996), and this work
$B^{v(0)}_{NH_4,ClO_4}$	−1.269e−3	4.137e−6		273–313	Linke (1965), Krumgalz et al. (1996), and this work
$B^{v(1)}_{NH_4,ClO_4}$	−3.329e−3	1.157e−5		273–313	Linke (1965), Krumgalz et al. (1996), and this work
$C^{v}_{NH_4,ClO_4}$	5.785e−4	−1.909e−6		273–313	Linke (1965), Krumgalz et al. (1996), and this work
$B^{v(0)}_{NH_4,NO_3}$	−9.102e−5	3.12e−7		273–288	Linke (1965), Krumgalz et al. (1996), and this work
$B^{v(1)}_{NH_4,NO_3}$	3.630e−3	−1.221e−5		273–288	Linke (1965), Krumgalz et al. (1996), and this work
$C^{v}_{NH_4,NO_3}$	−3.44e−8			273–288	Linke (1965), Krumgalz et al. (1996), and this work
$B^{v(0)}_{NH_4,HCO_3}$	8.20e−6			273–288	Linke (1965) and this work
$B^{v(1)}_{NH_4,HCO_3}$	2.25e−4			273–288	Linke (1965) and this work
$C^{v}_{NH_4,HCO_3}$	1.99e−6			273–288	Linke (1965) and this work
$B^{v(0)}_{NH_4,SO_4}$	−5.078e−5	2.76e−7		268–308	Linke (1965), Krumgalz et al. (1996), and this work
$B^{v(1)}_{NH_4,SO_4}$	2.334e−2	−7.81e−5		268–308	Linke (1965), Krumgalz et al. (1996), and this work
$C^{v}_{NH_4,SO_4}$	−3.931e−5	1.2853e−7		268–308	Linke (1965), Krumgalz et al. (1996), and this work
$\overline{V}^{(0)}_{NH_4}$	1.002813e2	−5.920729e−1	1.058741e−3	273–323	Millero (2001) and this work
$K^{(0)}_{NH_4}$	9.069507e−3	−1.181049e−5	−4.895105e−8	273–323	Millero (2001) and this work
$\overline{V}^{(0)}_{NH_3}$ [a]				176–303	Croft et al. (1988) and this work
$K^{(0)}_{NH_3}$	0.0			176–303	Croft et al. (1988) and this work

[a] $V^{(0)}_{NH_3} = 1.24519e-1T + 7.47828e-3P - 2.73705e-5TP - 1.45173e-4T^2$, where $P = (P_T - 1.01325)$.

Table 2
Equilibrium constants at 1.01325 bars (as $\mathrm{Ln}(K) = a_1 + a_2 * T + a_3 * T^2$) derived in the study (numbers are in computer scientific notation where e ± *xx* stands for $10^{\pm xx}$).

Solution–solid phase equilibrium	a_1	a_2	a_3	Temperature range (K)	Solid phase molar volume (cm^3/mole)	Data source
$NH_4Cl \Longleftrightarrow NH_4^+ + Cl^-$	−7.089666e0	3.568940e−2	−7.946733e−6	258–303	34.96	Linke (1965), Webmin[a] and this work
$NH_4ClO_4 \Longleftrightarrow NH_4^+ + ClO_4^-$	−3.781318e1	2.103026e−1	−2.839037e−4	270–307	60.25	Linke (1965), Lide (1994), and this work
$NH_4NO_3 \Longleftrightarrow NH_4^+ + NO_3^-$	−2.072302e1	1.310891e−1	−1.834524e−4	256–283	48.20	Linke (1965), Webmin[a], and this work
$NH_4HCO_3 \Longleftrightarrow NH_4^+ + HCO_3^-$	−3.654137e1	2.234553e−1	−3.389387e−4	269–313	50.04	Linke (1965), Lide (1994), and this work
$(NH_4)_2SO_4 \Longleftrightarrow 2NH_4^+ + SO_4^{2-}$	−1.664660e1	8.986410e−2	−1.126054e−4	254–303	74.74	Linke (1965), Webmin[a], and this work
$NH_3 \cdot H_2O \Longleftrightarrow NH_3 + H_2O$	6.170228e1	−6.730850e−1	1.952563e−3	173–188	37.50	Linke (1965), Leliwa-Kopystynski et al. (2002), and this work
$NH_3 \cdot 2H_2O \Longleftrightarrow NH_3 + 2H_2O$	−3.430372e0	3.551375e−2		175–176	55.11	Kargel et al. (1991) and Leliwa-Kopystynski et al. (2002)
$NH_3(g) \Longleftrightarrow NH_3(aq)$[b]	−8.09694e0	−3.14e−3	3.917507e3	273–313		Clegg and Brimblecombe (1989)
$NH_3 + H_2O \Longleftrightarrow NH_4^+ + OH^-$[b]	1.69732e1	−4.40e−2	−4.411025e3	273–313		Clegg and Brimblecombe (1989)

[a] http://webmineral.com.
[b] These two equations are defined as: $\mathrm{Ln}(K) = a_1 + a_2 * T + a_3/T$.

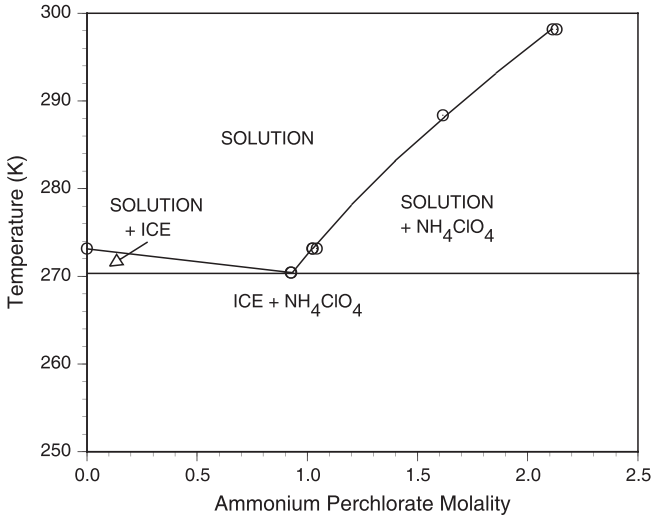

Fig. 2. Equilibrium of ammonium perchlorate in the 270–298 K temperature range. Symbols are experimental data; solid lines are model estimates.

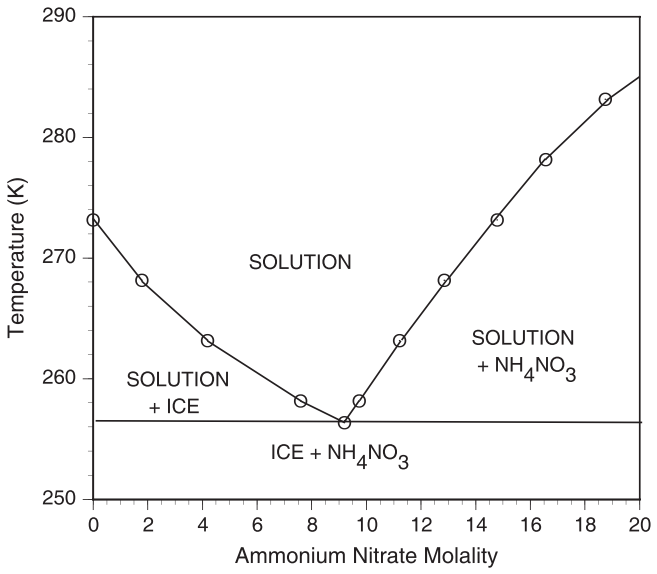

Fig. 3. Equilibrium of ammonium nitrate in the 256–285 K temperature range. Symbols are experimental data; solid lines are model estimates.

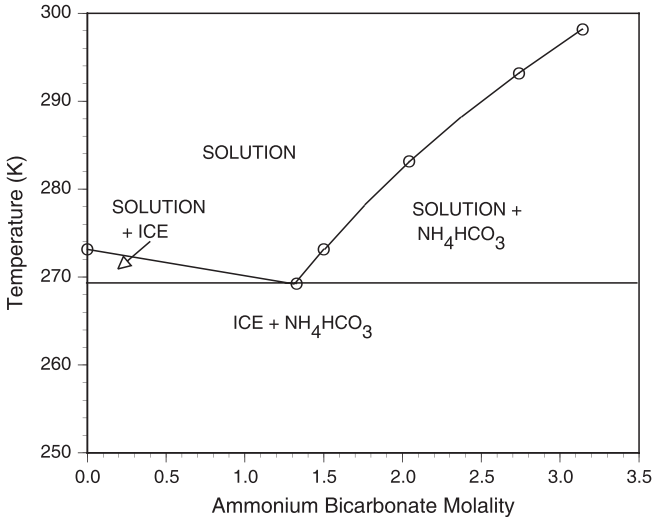

Fig. 4. Equilibrium of ammonium bicarbonate in the 269–298 K temperature range. Symbols are experimental data; solid lines are model estimates.

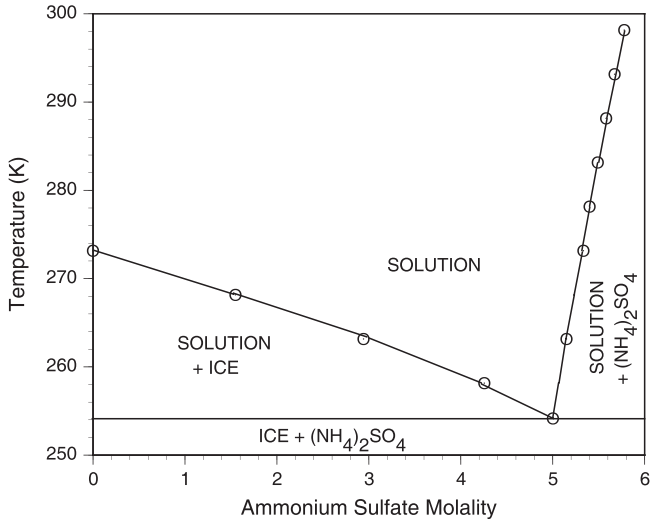

Fig. 5. Equilibrium of ammonium sulfate in the 254–298 K temperature range. Symbols are experimental data; solid lines are model estimates.

The Pitzer parameters for NH_4–SO_4 interactions at 298.15 K were taken from Pitzer (1991), and extended to lower temperatures by fitting $(NH_4)_2SO_4$–ice data from Linke (1965) (Fig. 5 and Table 1). Parameterization of the ice line to 254 K allowed us to estimate equilibrium constants for $(NH_4)_2SO_4$ (mascagnite) (Table 2). Our model estimate for the eutectic temperature and concentration of $(NH_4)_2SO_4$ were 254.15 K and 5.00 m, which are in excellent agreement with the literature values of 254.15 K and 5.00 m (Linke, 1965).

The lowest aqueous temperature that dealt with FREZCHEM in the past was 188 K (Marion, 2002). Ammonia solubility for FREZCHEM necessitates lowering the ice–H_2O(aq) level to at least 173 K. Fig. 6 shows the activity of water in equilibrium with ice and aqueous solutions (with salts) for the existing FREZCHEM model, which was largely developed from Clegg and Brimblecombe (1995). Also included in this figure is a similar equation developed by Swanson (2009). The lowest experimental temperature in the Clegg and Brimblecombe (1995) model was at 202 K, where the experimental a_w was 0.518; the FREZCHEM model (Fig. 6) calculates an $a_w = 0.521$ in close agreement with this experimental value. The Swanson (2009) equation, on the other hand, calculates $a_w = 0.540$ at 202 K. Because FREZCHEM seems in better agreement with the low experimental data, we retained using the FREZCHEM equation (Fig. 6) down to 173 K. But in cases where the temperature drops below 173 K (ammonia plus salts), the FREZCHEM model is programmed to use the Swanson equation (Fig. 6).

Binary parameters for the neutral NH_3(aq) component are summarized in Table 3, which are elements of Eqs. (1)–(3) and (5). Ammonia (Fig. 7) is generally much more soluble than ammonium salts (Figs. 1–5). For temperatures between 273 and 313 K, we relied upon equations developed by Clegg and Brimblecombe (1989) to assess the solubility of ammonia in pure aqueous and multicomponent solutions. For solutions in which ion concentrations are negligible (Eq. (3) without cations (c) and anions (a)), the activity coefficient for ammonia is given by

$$\gamma_{NH_3} = \exp(2m_{NH_3}\lambda_{NH_3,NH_3}) \quad (10)$$

where $\lambda_{NH_3,\,NH_3}(273\text{—}313\ \text{K})$ is given by

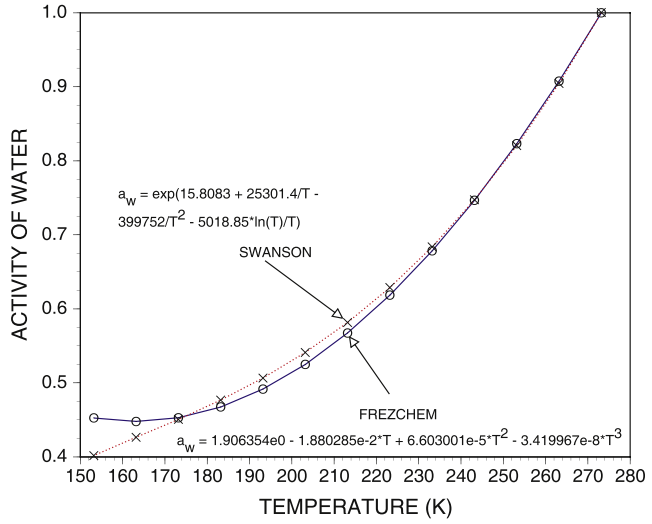

Fig. 6. A comparison of the model calculated activity of water (a_w) in equilibrium with ice and salts from the FREZCHEM model (Marion and Kargel, 2008) and from Swanson (2009). Symbols are experimental data; lines are model estimates.

Table 3
Aqueous NH_3 Pitzer-equation parameters used in this work (T = 298.15 K). (Clegg and Brimblecombe, 1989).

Pitzer-equation parameters	a_1
$\lambda_{NH3,Na}$	0.031
$\lambda_{NH3,K}$	0.0454
λ_{NH3,NH_4}	0.00
$\lambda_{NH3,Mg}$	−0.21
$\lambda_{NH3,Ca}$	−0.081
$\lambda_{NH3,Sr}$	−0.041
$\lambda_{NH3,Cl}$	0.00
$\lambda_{NH3,F}$	0.091
$\lambda_{NH3,Br}$	−0.022
λ_{NH3,ClO_4}	−0.056
λ_{NH3,NO_3}	−0.01
$\lambda_{NH3,OH}$	0.103
λ_{NH3,CO_3}	0.180
λ_{NH3,SO_4}	0.140

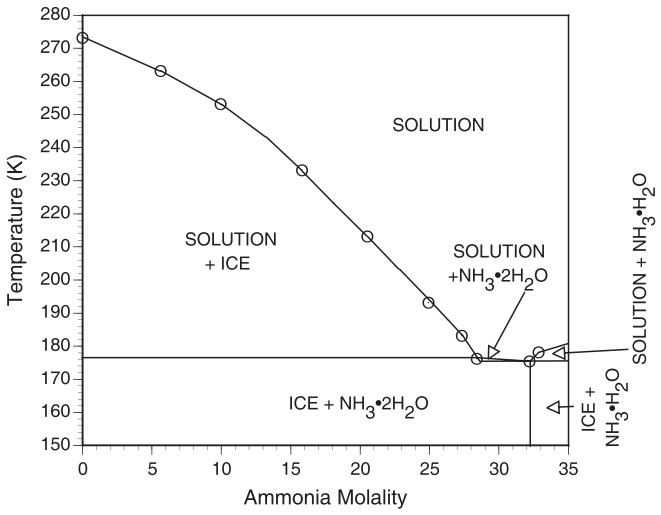

Fig. 7. Equilibrium of water–NH_3 system in the 173–273 K temperature range. Symbols are experimental data; solid lines are model estimates.

$$\lambda_{NH_3,NH_3} = 0.033161 - \frac{21.12816}{T} + \frac{4665.1461}{T^2} \quad (11)$$

(Clegg and Brimblecombe, 1989).

At subzero temperatures, we used the NH_3–ice line data (Fig. 7) from Linke (1965) to estimate the NH_3 activity coefficients (λ_{NH_3}). Pure ice formation as a function of T fixes the activity of water (a_w) and the osmotic coefficient (ϕ) in Eq. (4). In Eq. (5)(without cations (c) and anions (a)), the last term allows the calculations of λ_{NH_3,NH_3} (given ϕ), which enables Eq. (10) to calculate λ_{NH_3}. The derived λ equation for subzero temperatures (173–273 K) is given by

$$\lambda_{NH_3,NH_3} = 7.866587e-1 - 1.270466e-2T + 6.870081e-5T^2 - 1.211693e-7T^3 \quad (12)$$

Eq. (12) leads to an excellent fit to the experimental "ice" data in Fig. 7. Eq. (11) from Clegg and Brimblecombe (1989) presumably also leads to accurate values at higher temperatures. But at 273.15 K with NH_3(aq) = 1.0 m, Eq. (11) leads to $\lambda_{NH_3(aq)} = 1.037$, while Eq. (12) leads to $\lambda_{NH_3(aq)} = 0.947$. There is no way to reconcile this discrepancy. So as currently structured, Eq. (11) will be used for temperatures ⩾273 K, and Eq. (12) will be used for temperatures <273 K. For our icy body applications, temperatures <273 K are most critical, and Eq. (12) works best at these temperatures (Fig. 7).

Given estimates of λ_{NH_3} at subzero temperatures, two equilibrium constants were developed for the lower temperature range of $NH_3{\cdot}XH_2O$ (Fig. 7 and Table 2). The $NH_3{\cdot}H_2O$ solid phase was derived from Linke data (1965), and the $NH_3{\cdot}2H_2O$ was derived from Kargel et al. (1991). If we estimate the peritectic where ice and $NH_3{\cdot}2H_2O$ meet, our model predicts T = 176.2 K with NH_3(aq) = 28.7 m, which compares to the Kargel et al. (1991) values of T = 176.2 K with NH_3(aq) = 28.4 m.

The model was limited to NH_3(aq) = 35 m (Fig. 7). NH_3 is highly soluble eventually becoming 100% NH_3(aq). FREZCHEM is limited in its capacity to deal with high concentrations. Other examples, similar to NH_3, were HCl, HNO_3, and H_2SO_4 that were limited to 12 m, 9 m, and 8 m, respectively (Marion, 2002).

Two equilibrium constants not mentioned above were the Henry's law constant (NH_3(g)—NH_3(aq)) and the NH_3(aq)—NH_4(aq) constants that are listed in Table 2, and in all cases taken from Clegg and Brimblecombe (1989). The latter equation is listed in FREZCHEM as

$$K_{234} = \frac{(NH_4^+)(OH^-)}{(NH_3(aq))(H_2O)} \quad (13)$$

where parentheses refer to activities. If we combine and rearrange this equation with the water dissociation equation

$$K_{18} = \frac{(H^+)(OH^-)}{(H_2O)} \quad (14)$$

it leads to

$$H^+ = \frac{(NH_4^+)K_{18}}{(NH_3(aq))K_{234}} \quad (15)$$

an equation that allows an estimate of pH (=$-\log_{10}(H^+)$). For example, with NH_4Cl = 1.0 m and NH_3(aq) = 1.0 m, the pH values range from 9.48 at 298 K to 10.34 at 273 K. Extrapolating Eq. (15) to the eutectic for this case (175.45 K) (way beyond the range of Eq. (13), 273–313 K, Table 2) leads to a pH = 17.40, which may not be valid given the 98 K extrapolation of a non-linear equation from 273 to 175 K, but, nevertheless, will be used to approximate low temperature pH.

3.2. Density and pressure parameterization

The FREZCHEM model is structured to predict density and the effects of pressure on chemical equilibrium (Marion et al., 2005, 2008, 2009b; Marion and Kargel, 2008). Implementation of these equations requires a specification of the partial molar volume ($\overline{V}_i^0$) and compressibility (K_i^0) of individual aqueous species (e.g., NH_3 and NH_4^+) and binary Pitzer-equation volumetric parameters (e.g., B_{ca}^{ν}, Table 1).

Most of the volumetric Pitzer parameters at 298 K for NH_3 and NH_4^+ were taken from Krumgalz et al. (1996) and extended to lower and higher temperatures from Linke (1965) data. The molar volume and compressibility terms for NH_4^+ were taken from Millero (2001). The molar volume terms for NH_3 were developed from 955 data from Croft et al. (1988), and covers the temperature range of 176–303 K and the pressure range of 0–1000 bars.

Equation (6) is how density (ρ) is calculated in FREZCHEM. The $\overline{V}_i^0$ term is given in Table 1 and the V_{mix}^{ex} term is a function of the volumetric binaries in Table 1 (Eq. (7)). With these volumetric data and Eq. (6), it is possible to estimate the density of various solutions. Fig. 8 is an example for NH_4Cl and $(NH_4)_2SO_4$ saturated solution densities based on mineral data from Linke (1965). The experimental data is highly variable, especially for NH_4Cl that is based on different studies, but the model gives reasonable approximations of density (Fig. 8).

4. Validation and limitations

While model fits to experimental data are encouraging and point out the self-consistency of the model and data inputs (Figs. 1–5, 7 and 8), they are not validation, which requires comparison to independent data for multi-component solutions. Fig. 6 can be considered a validation check as the two equations that it compares for a_w–ice equilibrium were developed independently. Another independent check deals with activity coefficients at 298 K for NH_4Cl, NH_4NO_3, and $(NH_4)_2SO_4$ that were developed using the Pitzer equations (Eqs. (1)–(3)) that we compare to independent activity coefficients from Robinson and Stokes (1970) (Fig. 9). The concentrations in these cases range from 0.1 to 6.0 m for NH_4Cl and NH_4NO_3 and from 0.1 to 4.0 m for $(NH_4)_2SO_4$. There were minor differences between the two sets of activity coefficients at 1.0 m including −0.5% for NH_4Cl, 1.0% for NH_4NO_3, and 1.6% for $(NH_4)_2SO_4$. But in general, these two sets are in reasonable agreement (Fig. 9), which is important for application of ammonium salts.

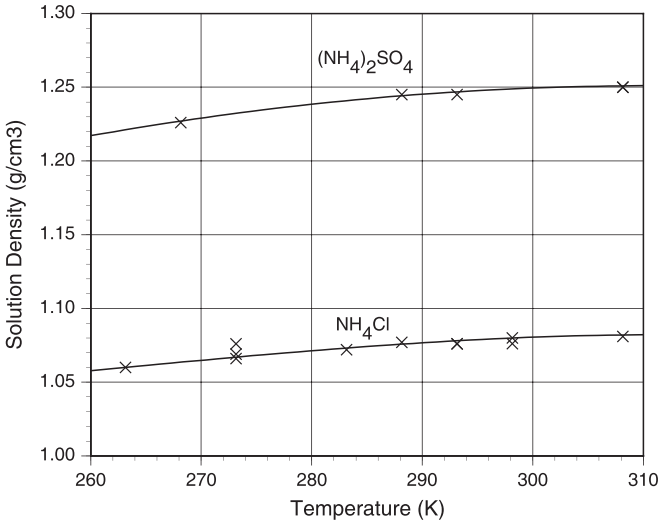

Fig. 8. Experimental data (Linke, 1965) (symbols) and model calculations (solid lines) of mineral-saturated NH_4Cl and $(NH_4)_2SO_4$ solution densities.

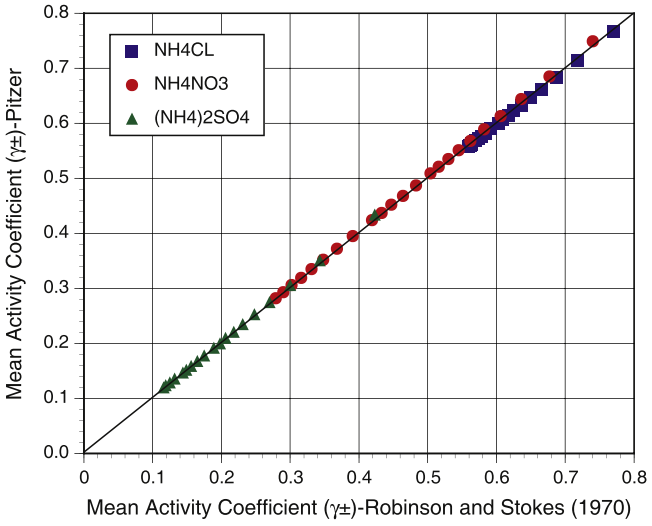

Fig. 9. A comparison of Pitzer model activity coefficients for NH_4Cl (0.1–6 m), NH_4NO_3 (0.1–6 m), and $(NH_4)_2SO_4$ (0.1–4.0 m) to experimental data from Robinson and Stokes (1970) at 298 K.

A potentially significant limitation of our ammonia–ammonium salt systems has to do with the solubility of NH_3(aq) versus NH_4^+. Figs. 1–5 show that eutectic temperatures ranged from 254 to 270 K for NH_4 with Cl^-, ClO_4^-, NO_3^-, HCO_3^-, and SO_4^{2-}. These temperatures are well above the peritectic of NH_3(aq), which is at 176 K (Fig. 7). In the following section, we will simulate down to NH_3(aq) eutectics, which will carry NH_4 and multiple other ions that have eutectics much higher in temperature than 176 K. How accurate these extensions to low temperatures are difficult to assess, but the model presented here provides the best estimates for multiple salts available at present.

In the simulations for Enceladus and Titan solution phases, we will calculate pH that has five options in FREZCHEM. Option 1 ignores pH (e.g., a NaCl + $(NH_4)_2SO_4$ case). Option 2 adds a fixed pH (e.g., pH = 8) to model calculations. Option 3 is based on the "acidity" (H^+) added to input. Option 4 is based on fixed "alkalinity" ($HCO_3^- + 2CO_3^{2-}$) added to input (Enceladus case). Option 5 is based on fixed ammonia and ammonium added to input (Eq. (15)); this option typically leads to especially high alkalinity (pH) values (Titan case). In the following Enceladus and Titan cases, we will largely focus on fractional crystallization that does not allow precipitates to re-dissolve, which allows more realistic examples for cold environments where ice and salts form and persist. But we will also compare an equilibrium crystallization example to fractional crystallization in Section 5.1 Enceladus.

5. Applications to outer planet moons

5.1. Enceladus

The *Cassini* mission discovered and explored a plume of gas and solid material originating from multiple jets emanating from near the south polar region of Enceladus (Porco et al., 2006; Waite et al., 2006, 2009, 2011; Fortes, 2007; Nimmo et al., 2007; Cooper et al., 2009; Postberg et al., 2009, 2011; Zolotov et al., 2011). Among the observations are the plume compositions (flyby E7) that Waite et al. (2011) expressed as weight ratios (e.g., grams of CO_2 per gram of plume, i.e., dimensionless). Their weight mixing ratios of H_2O, CO_2, NH_3, and CH_4 are 0.92 ± 0.03, 0.008 ± 0.003, 0.008 ± 0.003,

and 0.0021 ± 0.0009, respectively (Waite et al., 2011). We divided the above weight fractions of each species by molecular weights (g mol^{-1}) and multiplied by 1000 g l^{-1} to convert to approximate molarity, i.e., mol l^{-1} (e.g., H_2O = 51.07 mol l^{-1}, CO_2 = 0.1818 mol l^{-1}, CH_4 = 0.1309 mol l^{-1}, and NH_3 = 0.4697 mol l^{-1}), as though the plume was condensed as a liquid. These are easier units for comparison with FREZCHEM calculations that are based on aqueous phases. These are approximate molarities, as we have not used the densities of the solution but rather approximated the solution as being equal in density to pure water; we note that some soluble gases, such as CH_4, decrease the density of aqueous solutions, whereas others, such as CO_2, increase the density, and the total is probably not much different than 1 kg/l. The presence of salts, such as NaCl (0.05–0.20 mol kg^{-1}), and $NaHCO_3$ (or Na_2CO_3) (0.02–0.1 mol kg^{-1}) has been seen in both E-ring ice grains and in material emanating from the plume (Postberg et al., 2009, 2011).

In Table 4 are model approximations of these salts that will be used in our simulations. Clearly, the relative concentrations of CO_2 and CH_4 in the Enceladus plume are much higher than is possible based solely on aqueous phases (Waite et al., 2009); so we assumed that gas hydrates based on a mixture of CO_2 and CH_4 were also present. See Marion et al. (2006) for how gas mixtures were assigned in FREZCHEM. There may also be dry gas hydrates on Enceladus (Zolotov et al., 2011), but FREZCHEM requires that gas hydrates be in equilibrium with water, which is common on Earth. Included in Table 4 are gases that can approximate plume gas mixtures via gas hydrates. The gas data (initial values at 1 bar were CO_2(g) = 0.349 bars, CH_4 = 0.651 bars, and at 10 bars were CO_2(g) = 3.49 bars and CH_4(g) = 6.51 bars) were selected to simulate the plume gas ratios for CO_2 and CH_4. While CO_2 and CH_4 required something beyond the liquid phase to account for the plume composition, this is not the case for NH_3, which is much more soluble in liquid water (Fig. 7). So for NH_3, we assigned an initial value of 6.375e−5 m NH_3(aq), which was based on the plume gas ratios for CO_2 and NH_3. Below we will compare the model simulations to plume compositions.

Table 4
Initial compositions (Na, Cl, alkalinity) from Postberg et al. (2009) and model calculated gas components that will lead to Enceladus plume compositions (CO_2, CH_4, NH_3) (Waite et al., 2011) (Fig. 10).

Elements	Compositions
Na (mol/kg)	0.25
Cl (mol/kg)	0.20
Alkalinity (equil./kg)	0.05
CO_2(g) (bars)	0.349
CH_4(g) (bars)	0.651
NH_3(aq) (mol/kg)	6.375e−5
Temperature (K)	298.15
Pressure (bars)	1.0
pH (calculated)	6.76

If the data in Table 4 are inputted into FREZCHEM at 298 K, the calculated pH = 6.76, but nothing precipitates. But when we ran the simulation at 253 K under fractional crystallization, the case at 1.0 bar pressure led to the precipitation of $NaHCO_3$ and ice (Fig. 10). The CO_2 and CH_4 gas pressures did not rise to gas hydrate formation until the system reached 8.4 bars, where gas hydrates replaced ice as a sink for water. The amounts of CO_2 and CH_4 gas hydrates that precipitated at 8.4 bars were 5.98e−4 mol and 4.31e−4 mol, respectively. The relative contents of $CO_2{\cdot}6H_2O$/$CH_4{\cdot}6H_2O$ were 1.388 (5.98e−4/4.31e−4), which were in excellent agreement with the plume ratios of 0.1818/0.1309 = 1.389 (see initial paragraph in Section 5.1). The $CO_2{\cdot}6H_2O/NH_3$(aq) ratio for our simulation at 8.4 bars of pressure was 5.98e−4/1.54e−3 = 0.387, which was in excellent agreement with the plume ratios of 0.1818/0.4697 = 0.387 (see previous discussion).

At the point where gas hydrates formed at 8.4 bars of pressure under fractional crystallization (Fig. 10), the amount of residual water remaining in solution was 41.3 g. Running this same case under equilibrium crystallization, we ended up with exactly the same residual water (41.3 g) at 8.4 bars where the same gas hydrates formed. However, the amount of water associated with gas hydrates that formed under fractional crystallization was 0.1 g compared to the equilibrium crystallization where 958.7 g of water was associated with the gas hydrates. Ice formed under fractional crystallization (958.6 g) was not allowed to melt. But in a real environment under a pressure of 8+ bars, significantly more gas hydrates would form than was in this fractional 1–10 bar case. The reason we favor fractional crystallization is because in natural environments ice would float to the surface and salts would sink to the bottom making it difficult to bring all the input components together as is the case for equilibrium crystallization. For this reason, we generally use fractional crystallization in our natural simulations.

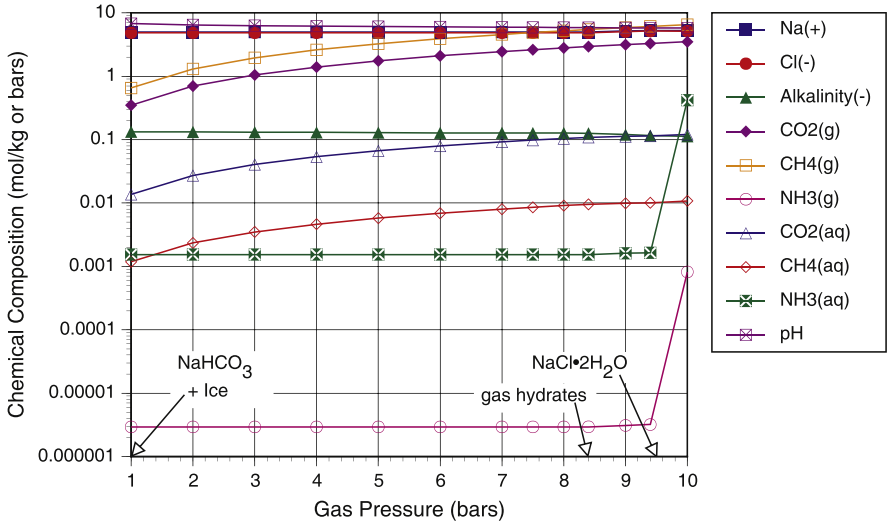

Fig. 10. The chemical compositions under fractional crystallization as gas pressures (CO_2 + CH_4) increase from 1 to 10 bars beneath Enceladus at 253 K. In this case, gas hydrates are a mixture of CO_2 and CH_4. Arrows on the *X*-axis indicate when solid phases start to precipitate. See Table 4 for the original compositions at 298 K.

These CO_2–CH_4–NH_3 values (Table 4 and Fig. 10) were only designed to approximate the relative concentrations of these constituents. Had we used a NH_3(aq) phase of 1.0 m, then the $CO_2{\cdot}6H_2O$/NH_3(aq) ratio at 8.6 bars, where $CO_2{\cdot}6H_2O$ first precipitates, would have been 0.00412/6.941 = 0.00059, which is considerably lower than the plume value of 0.387. NH_3 appears to be a minor constituent relative to CO_2 based on plume values (Waite et al., 2009, 2011). Also, not considered in our simulation was the role of CO_2(aq). The concentration of CO_2(aq) is about one order of magnitude higher than CH_4(aq) (Fig. 10), but still relatively low with respect to either gas concentrations or gas hydrate contents.

There are a few more points that are relevant to model simulations of Enceladus. In the gas pressure simulation (Fig. 10), the pH values ranged from 6.76 at 1 bar to 5.74 at 10 bars of pressure. These pH values are much lower than pH values suggested by earlier Enceladus simulations that were pH = 8–11 (Zolotov, 2007). Our simulations are lower in pH largely due to an aqueous alkaline phase under relatively high CO_2(g) concentrations (0.349–3.49 bars) that drives the solution to more acidic values. Another issue related to alkalinity is that the alkalinity temperature range is somewhat model limited by extrapolations below 273 K of Henry's law constant [CO_2(aq)/CO_2(g)], and the first bicarbonate [(H)(HCO_3)/(CO_2(aq))(H_2O)] and second carbonate [(H)(CO_3)/(HCO_3)] dissociation constants (Marion, 2001). There is a scattering of some bicarbonate (e.g., $NaHCO_3$) and carbonate (e.g., $Na_2CO_3{\cdot}10H_2O$) chemistries to 251 K in FREZCHEM; but extrapolations below about 250 K would be limited. At 8.4 bars of pressure in this specific case, 89.6% of the original bicarbonate (0.05 m, Table 4) precipitated at 253 K. So if extrapolation to lower temperatures than 253 K were necessary, we would probably remove the alkalinity as has been done in the past (Marion et al., 2010a). The last solid phase to precipitate in this simulation was hydrohalite ($NaCl{\cdot}2H_2O$) at 9.5 bars (Fig. 10). By the time the system reached 10 bars, all elements in this simulation (Table 4) were precipitating as solid phases, except for NH_3(aq), which is what caused the sharp spike in ammonia components between 9.4 and 10 bars (Fig. 10). By the time the system reached 10 bars, the bulk of the water (1000 g) precipitated as ice (958.6 g), gas hydrates (34.1 g), and $NaCl{\cdot}2H_2O$ (7.2 g) with ≈0.15 g H_2O remaining in solution.

5.2. Titan

There have been numerous studies in recent years dealing with the chemistries of subsurface fluids on Titan, especially with respect to $(NH_4)_2SO_4$, NH_3, and $CH_4{\cdot}6H_2O$ (Osegovic and Max, 2005; Atreya et al., 2006; Fortes et al., 2007; Spencer and Grinspoon, 2007; Grindrod et al., 2008; Sohl et al., 2010; Norman and Fortes, 2011; Fortes, 2012). Theory suggests that there may be subsurface water oceans on Titan (Fortes, 2000; Baker et al., 2005; Tobie et al., 2005; Fortes et al., 2007; Lorenz et al., 2008; Sotin and Tobie, 2008; Sohl et al., 2010) that are today as close to 50 km of the surface and for much of the past may have been within 10–20 km (Tobie et al., 2005).

Table 5
Initital compositions for an early Titan subsurface chemistry (Fig. 11).

Elements	Compositions
NH_4 (mol/kg)	3.00
Cl (mol/kg)	1.00
SO_4 (mol/kg)	1.00
CH_4(g) (bars)	5.00
NH_3(aq) (mol/kg)	10.00
Temperature (K)	273.15
Pressure (bars)	10.0
pH (calculated)	11.24

The starting chemistries used in our Titan simulations are listed in Table 5 and reflect the above specified Titan chemistries ($(NH_4)_2SO_4$, NH_3, $CH_4{\cdot}6H_2O$), albeit the initial concentrations are arbitrary, which is different from the Enceladus case where initial compositions (Table 4) were constrained to predict plume gas compositions. The total pressure (10 bars) was used to include gases such as CH_4 and NH_3, and was designed to represent early Titan when a water ocean may have existed on the surface. After we discuss this initial simulation, we will present two cases where the total pressure was either 250 bars (≈20 km of ice depth) or 1000 bars (≈80 km of ice depth), and another case where NH_3(aq) was assigned 0.1 m compared to the 10.0 m (Table 5).

Our simulation ran from 273 K to 173 K (Fig. 11) at fractional crystallization (Table 5). The first solid phase to precipitate was $(NH_4)_2SO_4$ that started at 273 K. Later ice began to form at 241 K; the high concentration of NH_3(aq) (10.0 m) kept ice from forming early. At 226 K, the methane gas hydrate ($CH_4{\cdot}6H_2O$) began forming; at which point, ice stopped precipitating. The last solid to form was NH_4Cl at 206 K. At 173 K, $CH_4{\cdot}6H_2O$ was still forming, but the system was approaching equilibrium with $NH_3{\cdot}2H_2O$.

The anions, Cl and SO_4, started at 1.0 m, but $(NH_4)_2SO_4$ precipitated early and SO_4 dropped to low concentrations, while Cl (and NH_4) kept to relatively high solution-phase concentrations from 273 to 173 K (Fig. 11). We used CH_4(g) as a constant input (Table 5 and Fig. 11), which led to a rapidly increasing CH_4(aq) as temperature dropped, which eventually led to $CH_4{\cdot}6H_2O$ formation. The precipitation of methane hydrates ($CH_4{\cdot}6H_2O$) and the presence of soluble methane (CH_4(aq)) could serve as the source of atmospheric CH_4(g) or liquid CH_4(aq) that are common on the surface of Titan today (Mahaffy, 2005; Atreya et al., 2006; Tokano et al., 2006; Mitri et al., 2007; Stofan et al., 2007; Sotin, 2007; Lorenz, 2008). In particular, methane is known to be destroyed by photolysis on a geological short timescale of some tens of millions of years. So there must be a subsurface source of methane to replenish the atmosphere, which could be a gradual leak from crustal or oceanic methane clathrate. The methane clathrate is buoyant with respect to all the other solid phases (see below). NH_3 input was as NH_3(aq) and not NH_3(g) for a good reason in this case. Assigning an initial NH_3(aq) = 10.0 m led to a significant drop of NH_3(g) with temperature decrease (Fig. 11) that was calculated from NH_3(aq) and the Henry's law constant (Table 2). Had we specified NH_3(g) as our input, instead of NH_3(aq), then NH_3(aq) would have "exploded" in concentration. For NH_3(g) = 0.1 bars at 273 K, the NH_3(aq) would be 9.6 m; for NH_3(g) = 0.1 bar at 263 K, the NH_3(aq) would be 50.6 m, which is beyond the model limit of NH_3(aq) = 35 m (Fig. 7).

This case was developed to simulate an early Titan when temperatures would have been higher than today. Such an aqueous solution would first have precipitated $(NH_4)_2SO_4$ that would have fallen to the bottom of the ocean. Then as temperature declined, eventually ice would have formed that would have floated to the surface forming an ice layer with density = 0.9168 g cm^{-3}. The formation of $CH_4{\cdot}6H_2O$ would also float up to the ice layer because it has a lower density (0.9144 g cm^{-3}) than the brine layer (0.9849 g cm^{-3} at 241 K). This relatively low brine-layer density (<1.0 g cm^{-3}) is because the major solution constituents in this case were NH_3(aq) and NH_4^+ (Fig. 11). Next NH_4Cl would have formed and sank to the bottom of the ocean. As the above lightweight constituents moved upward, eventually $NH_3{\cdot}2H_2O$ (or $NH_3{\cdot}H_2O$) would likely have precipitated assuming the temperature reached ≈176 K or lower. However, if the ocean persists on Titan today, formation of $NH_3{\cdot}2H_2O$ may not be a prevalent solid phase on Titan.

As pointed out earlier, we also ran a similar simulation at 250 bars of pressure (Table 5), which represents ≈20 km of ice, analogous to Europa (Marion et al., 2005; Marion and Kargel,

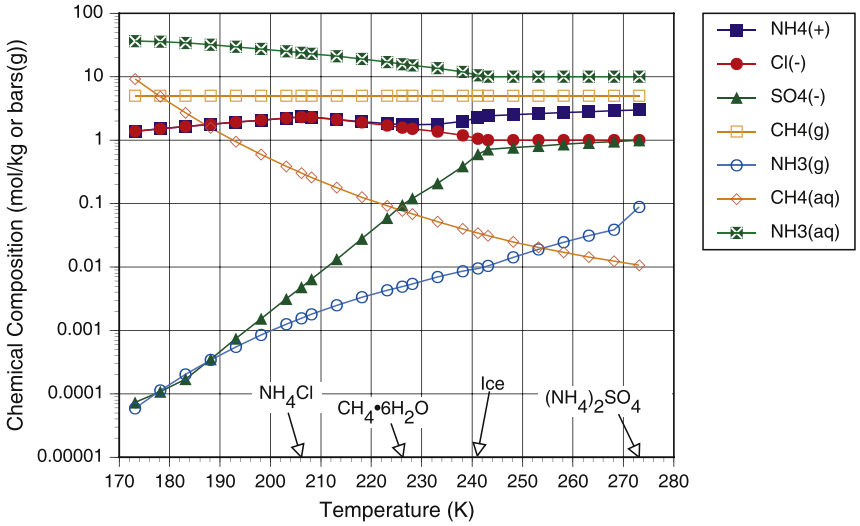

Fig. 11. The chemical compositions under fractional crystallization as temperature decreases from 273 to 173 K beneath an early Titan at 10 bars. Arrows on the *X*-axis indicate when solid phases start to precipitate. See Table 5 for the original compositions at 273 K.

2008). Such shallow oceans may have been present on Titan in the recent past, or even at present (Tobie et al., 2005; Norman and Fortes, 2011). This simulation caused $(NH_4)_2SO_4$ to start precipitating at 273 K, ice to start precipitating at 241 K, $CH_4{\cdot}6H_2O$ to start precipitating at 209 K, and NH_4Cl to start precipitating at 203 K. The largest difference between these two simulations was in the formation of $CH_4{\cdot}6H_2O$, which started respectively at 226 K at 10 bars of pressure (Fig. 11) and 209 K at 250 bars of pressure. At 173 K, $NH_3{\cdot}2H_2O$ is closer to formation at 250 bars of pressure than was the case at 10 bars of pressure. At a simulation of 1000 bars of pressure (≈80 km of ice), $(NH_4)_2SO_4$ forms at 273 K, ice, in this case, never forms, but $CH_4{\cdot}6H_2O$ starts forming at 239 K, and NH_4Cl forms at 214 K. The reason that $NH_3{\cdot}2H_2O$ never precipitates in the three Titan simulations is that $CH_4{\cdot}6H_2O$ formation keeps the activity of water (a_w) at a too low level for $NH_3{\cdot}2H_2O$ or $NH_3{\cdot}H_2O$ to precipitate. If CH_4(g) is removed in Table 5 and Fig. 11 simulation, $NH_3{\cdot}2H_2O$ precipitates at 175.45 K.

We also ran a simulation at a lower NH_3(aq) = 0.1 m. In this case at 173 K, the amount of liquid water was 2.76 g (from the initial value of 1000 g) compared to NH_3(aq) = 10 m, where the amount of liquid water was 276 g. A 100-fold difference in NH_3(aq) led to a 100-fold difference in liquid water. Otherwise, the patterns of 0.1 m NH_3(aq) were similar to Fig. 11 with respect to the solid phases that precipitated, albeit not exactly at the same temperatures. The pH values at 273 for 0.1 and 10.0 m NH_3(aq) cases were 9.08 and 11.24, respectively. The pH values at 173 K for 0.1 and 10.0 m NH_3(aq) cases were both 18.03; also both NH_3(aq) molalities had identical values at 173 K of 36.3 m. pH values of 18.03 at 173 K for both NH_3(aq) cases may not be accurate as pointed out in Section 3.1 with respect to Eq. (15). The reason we chose NH_3(aq) = 10.0 m as our main Titan case (Table 5 and Fig. 11) was because the low water levels for NH_3(aq) = 0.1 m (e.g., 2.76 g at 173 K, see above), due to high ice formations, led to convergence problems at lower temperatures. This, for example, was a problem for running NH_3(aq) = 0.1 m at 250 and 1000 bars.

6. Discussion

In the simulations, we compared Enceladus and Titan based largely on chemistries that are considered most likely prevalent on these moons today (Tables 4 and 5). But clearly the plumes of Enceladus are a more accurate source of subsurface, maybe ocean, chemical data than the atmospheres and surfaces of Titan. On the other hand, both Enceladus and Titan are projected to include gas hydrates of $CO_2{\cdot}6H_2O$ and/or $CH_4{\cdot}6H_2O$, or a mixed gas hydrates. Because of the low aqueous solubility of both CO_2(aq) and CH_4(aq) at moderate temperatures (253 K) (Figs. 10 and 11), the plumes of Enceladus and the atmosphere of Titan are difficult to understand unless there are gas hydrates or massive gas concentrations beneath their surfaces. On the other hand, if the liquid phases drop to low temperatures (<200 K), these aqueous solutions such as CH_4(aq) in Fig. 11 can rise to high levels and eventually liquid methane will form on the surface of Titan. Quantifying the subsurface temperature regimes would be very useful for simulation modeling.

Could the Enceladus simulated environment support life as we know it on Earth. The pH range for life on Earth is from −0.06 to maybe as high as 12.5–13 (Marion and Kargel, 2008). The model-calculated pH values between 1 bar and 10 bars of gas pressure in Fig. 10 ranged from 6.76 to 5.74, which is a perfectly good range for life on Earth. The high P_{CO2} values from 0.35 bars to 3.5 bars are the reason these examples have relatively low pHs for an alkaline case. The lower temperature level for active life, not dormant life, is approximately 253 K (Marion and Kargel, 2008), which was the temperature that we ran our simulation (Fig. 10). Given the inferred surface temperatures at the Enceladus plume source of 190 K (Spencer and Grinspoon, 2007; Kieffer and Jakosky, 2008), such a high temperature (253 K) may exist not far below the Enceladus surface perhaps within 20 km, which is quite feasible based on a Europa case (Marion et al., 2005; Marion and Kargel, 2008). The activities of water (a_w) in these 1–10 bar pressure simulations ranged from 0.82 to 0.80, which are well below Earth oceans that have an a_w = 0.98. The most extreme a_w value that supports life on Earth is ≈0.60 (Grant, 2004; Marion and Kargel, 2008). A salt-tolerant species could survive at these a_w values on Enceladus; that is, life could tolerate the chemical cases in this Enceladus simulation, even if not an optimal environment for life on Earth.

Could the Titan simulation based on Table 5 input support life as we know it on Earth? The pH range in the NH_3(aq) = 10 m simulation starts at 273 K with pH = 11.24 and ends at 173 K with pH = 18.03. Alkalinity, due to bicarbonate in the Enceladus case, was not a component of the Titan simulation. Instead pH was calculated with Eq. (15) that is a function of NH_4^+(aq) and NH_3(aq) activities; Eqs. (13) and (14) explain how Eq. (15) was developed. A potentially severe limitation of this calculation is that Eq. (13)

is only defined for temperatures: 273–313 K (Table 2). As pointed our earlier, life may tolerate pH values that rise to 12.5–13. The model-calculated pH = 13.0 is reached at 238 K. These high alkaline systems would require adaptable species that are rare on Earth. Temperatures in this case ran from 273 to 173 K, with an Earth active life limit of 253 K (Marion and Kargel, 2008). Assuming Titan behaves similarly to a Europa example (Marion et al., 2005; Marion and Kargel, 2008), with a surface temperature on Titan of 94 K (Coustenis, 2007), this could place a subsurface ocean temperature at 250 K with 240 bars of pressure, approximately 20 km beneath the surface. So assumptions that oceans on Titan might exist within a few tens of kilometers of the surface (Tobie et al., 2005; Beghin et al., 2010; Norman and Fortes, 2011) is possible and with respect to temperature could support life as we know it on Earth. The activity of water (a_w) (Fig. 11) starts at 0.72 at 273 K, drops to 0.605 at 223 K, and finally to 0.280 at 173 K. As pointed out earlier, $a_w \approx 0.60$ is the lower limit for life on Earth. The low limits for a_w in this Titan case are primarily due to CH_4 species. Eliminating CH_4 from this simulation leads to $a_w = 0.603$ at 220 K and $a_w = 0.455$ at 175.45 K. As was the case for the Enceladus simulation, the Titan simulation could also tolerate life as we know it on Earth, although at present might be confined to a depth around 45 km based on a model of the thermal evolution of the interior (Beghin et al., 2010).

In the simulations, we compared pH and a_w as limiting factors for life. The model calculations for pH on Enceladus (Fig. 10) ranged from 5.74 to 6.76, and similar calculations for Titan (Fig. 11) ranged from 11.24 to 18.03. The carbonate alkalinity ($HCO_3^- + 2CO_3^{2-}$) of Enceladus at high CO_2(g) levels kept the pH in a more favorable level than on Titan. But if we decrease the NH_3(aq) level on Titan from 10.0 to 0.1 m, then the pH ranged from 11.24 at 273 to 15.51 at 200 K versus 9.08 at 273 K and 15.79 at 0.1 m NH_3(aq). So at least at higher temperatures, lower NH_3(aq) values should be more favorable for life on a highly alkaline Titan, but still not as favorable as a less alkaline Enceladus. But this pH comparison assumed a higher alkalinity on Titan due to the presence of NH_3(aq) and NH_4^+(aq) (Table 5, Eq. (15)) compared to the lower alkalinity due to carbonate phases on Enceladus (Table 4). The a_w on the Enceladus simulation (Fig. 10) ranged from 0.80 to 0.82, and the a_w on Titan (Fig. 11) ranged from 0.28 to 0.72. Given that the lower limit for life on Earth is $a_w \approx 0.60$, Enceladus could be more favorable for life than Titan. In the past there have been arguments for why Titan, given an early environment similar to Earth, could be a highly favorable body in our Solar System for life (Margulis et al., 1977; Schulze-Makuch and Grinspoon, 2005). But if Titan oceans are highly alkaline with high pH and low a_w values, Enceladus would seem a better environment for life as we know it on Earth.

7. Cautions and future directions

Here we consider some cautions, one being an issue of relevance, and the others being issues of omission in the present parameterization of FREZCHEM.

7.1. Issue of relevance

Kargel (1991, 1992) and Kargel et al. (2000) proposed the relevance of sulfates, including ammonium sulfates, in icy satellites and chondrite-derived brines. This suggestion faces challenges from the presence of abundant sulfides in carbonaceous chondrites, from closed-system chemistry under reducing conditions, and from a suggested terrestrial contamination origin of chondrite sulfates (Zolensky et al., 1989, 1993, 1997; McKinnon and Zolensky, 2003).

A pre-terrestrial origin of CM chondrite sulfates has been supported both by the early investigators who documented sulfate veins and nodules in carbonaceous chondrites (e.g., Bostrom and Fredriksson, 1964; Fredriksson and Kerridge, 1988; Burgess et al., 1991), and by more recent oxygen isotopic analysis of sulfates in CM chondrites (Airieau et al., 2005). Airieau et al. (2005) were equivocal on the pre-terrestrial versus terrestrial origin of sulfates in CI chondrites. Gounelle and Zolensky (2001) considered the sulfate veins in CI chondrite Orgueil to have likely terrestrial origins, but they considered it possible that these veins either are terrestrially remobilized pre-terrestrial sulfates, or terrestrially oxidized and remobilized preterrestrial sulfides. In fact, aqueous phase equilibria show that any preterrestrial meridianiite ($MgSO_4{\cdot}11H_2O$) would have undergone deliquescence and recrystallization as lower hydrates, probably of epsomite ($MgSO_4{\cdot}7H_2O$) and/or hexahydrite ($MgSO_4{\cdot}6H_2O$) or even kieserite ($MgSO_4{\cdot}H_2O$), under prevailing terrestrial conditions.

If starting with a possible sulfide-bearing chondritic precursor lacking initial sulfates, there are pathways to a sulfate-rich aqueous system (as the carbonaceous chondrites show). Zolotov and Shock (2001) first considered thermodynamically the oxidation of sulfide-bearing chondrite-like material in Europa to form a sulfate-rich ocean; the process is possible if conditions involved hydrothermal conditions warmer than 323 K. Hydrogen production and loss is a key process. This proposed process extends a recurrent theme of planetary science where hydrogen production and loss from chondritic precursors drives oxidation (e.g., Dreibus and Wanke, 1987; Rosenberg et al., 2001).

Zolotov (2009) and Zolotov and Kargel (2009) consider sulfates to be likely major components of an aqueously altered Ceres and of a sulfate ocean of Europa, but hydrogen blow-off is a key requirement. McKinnon and Zolensky (2003) also favor a sulfate-rich ocean of Europa but have a very different evolutionary history than considered by Kargel (1991); they modeled an oxidizing, sulfate-rich ocean arising long after its origin, which could be consistent with the model of Zolotov and Shock (2001).

We must consider the cause, time, and place of origin of sulfates in carbonaceous chondrites to be an important unresolved set of issues. By extension, our assumed relevance of abundant sulfates (including ammonium sulfates and related chemistry) in carbonaceous chondrite-derived brines, such as may occur in Europa's ocean (Kargel et al., 2000) and other outer Solar System planetary bodies, should be considered a hypothesis and premise rather than established knowledge.

7.2. Ammonium carbonate species

Here we describe some key omissions in the current FREZCHEM and conditions under which the omitted components may be important. In the treatment above, and as encountered often in the planetary science literature, CO_2, NH_3, and H_2O coexist together. There are narrow conditions under which each is abundant together, but for the most part this system involves high reactivity (Kargel, 1992). The ternary system (Fig. 12) includes the pure end-members, ammonia hydrates, CO_2 clathrate hydrate ($CO_2{\cdot}5^3/_4H_2O$), ammonium carbonate ($(NH_4)_2CO_3$), ammonium carbamate (H_2N–$COONH_4$), ammonium carbonate monohydrate ($(NH_4)_2CO_3{\cdot}H_2O$), ammonium bicarbonate (NH_4HCO_3), a binary phase of ammonium bicarbonate and ammonium carbonate, and the pseudo-ternary urea ($CO(NH_2)_2$); FREZCHEM currently does not contain the latter five solids.

In the H_2O–CO_2–NH_3 ternary system, a given mixture will determine its own pH, depending on stoichiometry. When silicates or metal oxides or sulfates are added and abundant in the system, external buffers can impose a pH that drives the equilibrium. Under certain circumstances, with special stoichiometric ratios of materials (with or without added rocks) and specific narrow temperature intervals, free aqueous CO_2 and NH_3 can coexist together, each abundant. However, these conditions are narrow and might

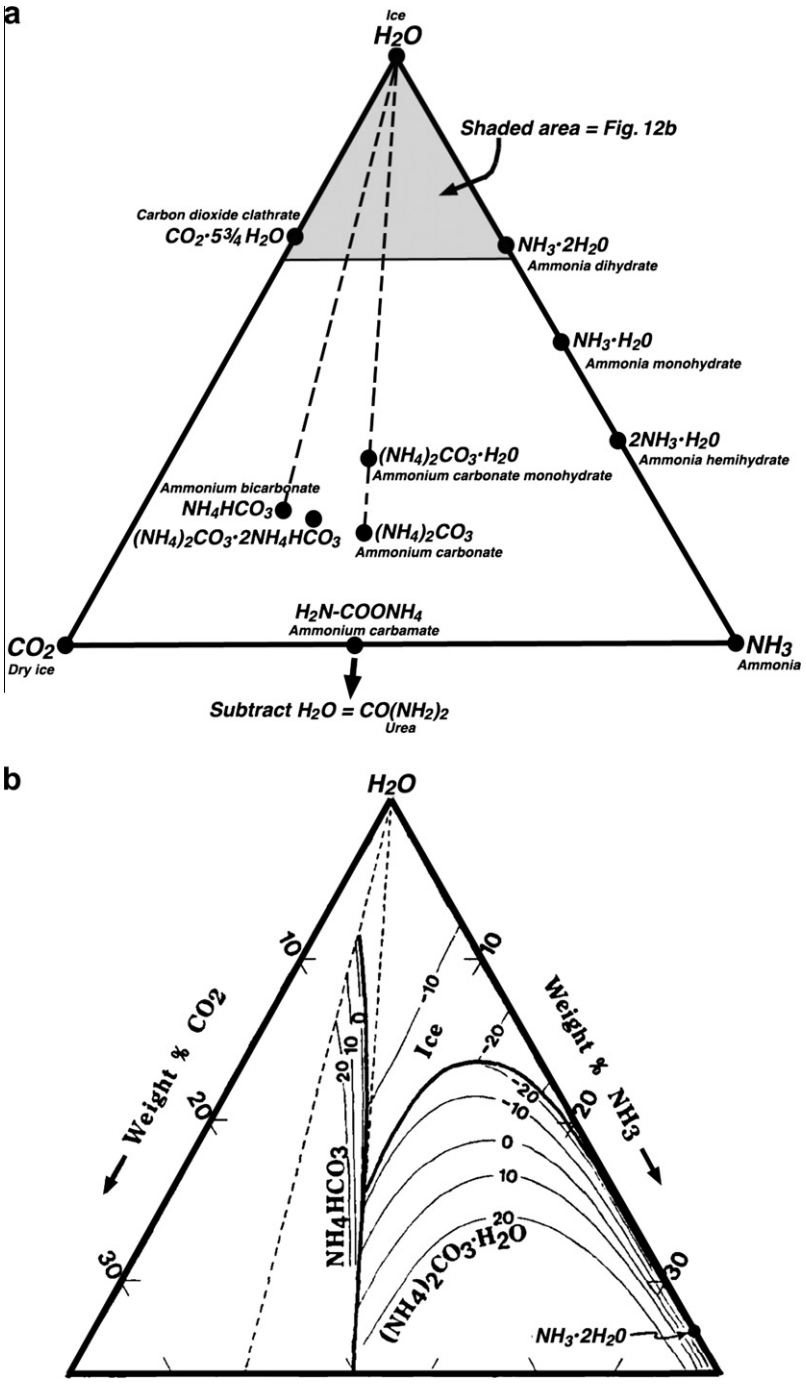

Fig. 12. Ternary system H_2O–NH_3–CO_2, (expressed by mass). (a) Solid compositions in the ternary system. Urea exists outside this ternary due to the subtraction of one water molecule from stoichiometric ammonium carbamate. (b) Liquidus of the water-rich end of the system, after Kargel (1992) from published data and his own experimental data at 1 atm total pressure. Liquidus temperatures are contoured in °C from −20° to +20 °C; the isotherms crowd together irresolvable below −20 °C. The two dashed lines in both panels isolate stoichiometric ratios of the ternary system separating physicochemical totally different types of liquids and solid assemblages. For example, free ammonia–water liquids (containing some ammonium carbonate component) can exist only to the ammonia-rich side of the right-hand dashed line; only these liquids can evolve by freezing to where ammonia dihydrate can exist in the solid assemblage with water ice and ammonium carbonate monohydrate. This ternary system, with planetary interpretations and deficiencies in knowledge, is discussed in more detail by Kargel (1992).

not be buffered such that both free ammonia and free carbon dioxide are simultaneously abundant. A wider range of situations has one as a major species; the other is commonly negligible. We note that although some comets and the plumes of Enceladus emit both carbon dioxide and ammonia, ammonia is a minor (verging on trace) component, whereas carbon dioxide is one to two orders of magnitude more abundant.

In terms of Fig. 12, Enceladus' plumes, and also most comet volatiles, project near the water apex and far toward the CO_2–H_2O join; thus, when solidified, these volatile assemblages would appear to project in the solid ternary phase space of ice + CO_2 clathrate + ammonium bicarbonate. To get into the region where free ammonia–water liquids would be produced by melting, it would be necessary to greatly increase the NH_3:CO_2 ratio. However, the full system phase equilibria are not known, to our knowledge. Herein, we suggest a worthy investigation.

As Kargel (1992) pointed out, the reaction kinetics favor formation of the ternary compounds even at temperatures as low as

195 K, though the reaction may take many hours to proceed at that temperature. Reaction kinetics at very low temperatures near most icy satellite surfaces are unknown, but may be vanishingly slow.

Kargel (1992) emphasized the incompatibility of free ammonia–water liquid with cometary volatiles. Comets have so little ammonia that free ammonia–water liquids are not apt to exist for long when comets are heated at perihelion. On the other hand, in some classical nebula models, NH_3:CO_2 ratios are so high that ammonia–water liquids are predicted (Lewis, 1972). Kargel (1992) suggested that a powerful exothermic reaction between the cometary volatiles formaldehyde and ammonia (forming hexamethylenetetramine) might power some comet outbursts and splitting. Maybe such reactions are why ammonia is so minor or absent in most observed Solar System icy bodies.

The reactivity of aqueous CO_2 and NH_3 is evident in the vapor partial pressures as these volatiles are mixed at ordinary temperatures (e.g., Fig. 13 of Que and Chen (2011)). With possibilities for important exceptions, as a general rule when ammonia–water liquids are encountered in our Solar System, or when CO_2-saturated aqueous liquids occur, CO_2 and NH_3 will not be simultaneously abundant.

7.3. Ammonium silicates

Ammonium ion NH_4^+ (ionic radius r = 1.43 Å) readily replaces K^+ (r = 1.33 Å) and Rb^+ (r = 1.47 Å) in crystalline silicate lattices and, to a minor extent, may also replace Na^+ (r = 0.97 Å). A typical reaction involving the K-feldspar component of plagioclase may be

$$KAlSi_3O_8 + NH_4^+(aq) \Longleftrightarrow NH_4AlSi_3O_8\ (\text{buddingtonite}) + K^+(aq) \quad (16)$$

High-grade metamorphic conditions experimentally have formed and decomposed buddingtonite (Voncken et al., 1993), an ammonium feldspar, at temperatures far out of range of FREZCHEM but demonstrating the high stability of this mineral:

$$2NH_4AlSi_3O_8 \Longleftrightarrow 2NH_3 + H_2O + Al_2O_3 + 6SiO_2 \quad (17)$$

Ammonium silicates are not very common on Earth. Barker (1964) thought this to be because ammonium-rich Earth environments are rare, but they might be common extraterrestrial. Ammonium silicates on Earth are primarily associated with siliceous hydrothermal and meta-sedimentary rocks. Ammonium silicates in the mantle are thought to have supplied N_2 and NH_3 to the primordial atmosphere (Eugster and Munoz, 1966; Andersen et al., 1995; Watenphul et al., 2010). Direct evidence for ammonium silicates in the modern mantle includes ammonium in lamprophyres (Wu et al., 2004).

Ammoniacal hydrothermal brines (< 500 ppm NH_4^+) sometimes completely replace plagioclase with buddingtonite (Barker, 1964; Erd et al., 1964). Most natural occurrences of buddingtonite and other ammonium silicates are in hydrothermally altered rocks, and primarily in gold- and/or mercury-hosting rocks and shales (Bottrell and Miller, 1990; Krohn et al., 1993; Voncken et al., 1993). In the Carlin gold ore deposits (Nevada), buddingtonite is locally abundant and even dominates one massif 8 km across. The common association with mercury has motivated general speculations that ammonium silicate forming environments usually involve late-stage vapor efflux from magmatic/hydrothermal bodies.

Terrestrial ammonium phyllosilicate minerals include varieties of muscovite, biotite, illite, montmorillonite, and many others (Vedder, 1965; Duit et al., 1986; Juster et al., 1987). Experimental synthesis of ammonium minerals mainly requires 600–800 K (Levinson and Day, 1968; Bos et al., 1988); they decrepitate at slightly higher temperatures. However, natural ammonium minerals indicate that NH_4^+ ion exchange occurs at very-low-grade metamorphic or diagenetic conditions (Juster et al., 1987), and together with the persistence of ammonium silicates in ancient high-grade metamorphic rocks, natural occurrences indicate a wide physicochemical stability. Ammonia–water cryovolcanic liquids could contain 3–5 orders of magnitude more ammonia than modern terrestrial groundwaters and hydrothermal brines. Spectroscopic evidence of ammonium minerals on extraterrestrial objects is limited and controversial at best, but this could be due to low abundances rather than absence of ammonium, or it could be due to the reactions taking place internally, such that the products are not visible on the surface. King et al. (1991) identified spectroscopically what they thought was an ammonium mineral on the carbonaceous asteroid I Ceres (King et al., 1991). Rivkin (1997) further suggested an ammoniated smectite on Ceres. However, Rivkin et al. (2006), while not dismissing the possibility of ammonium minerals on Ceres, suggested that iron phyllosilicates are a better explanation for the spectral features thought previously to be due to ammonium.

8. Conclusions

The main conclusions of this study were:

(1) For the new FREZCHEM version, Pitzer parameters, volumetric parameters, and equilibrium constants for the Na–K–NH_4–Mg–Ca–Fe(II)–Fe(III)–Al–H–Cl–ClO_4–Br–SO_4–NO_3–OH–HCO_3–CO_3–CO_2–O_2–CH_4–NH_3–Si–H_2O system were developed for ammonia and ammonium compounds that cover the temperature range of 173–298 K and the pressure range of 1–1000 bars.

(2) Ammonia solubility extends to 173 K, where $NH_3{\cdot}2H_2O$ and $NH_3{\cdot}H_2O$ precipitate, which is the lowest temperature in existing FREZCHEM versions.

(3) A subsurface "ocean" on Enceladus was simulated at 253 K with gas pressures, 1–10 bars, and with Na^+, Cl^-, HCO_3^-, $CO_2(g)$, $CH_4(g)$, and $NH_3(aq)$ that led to precipitation of ice, $NaHCO_3$, and gas hydrates ($CO_2{\cdot}6H_2O$ and $CH_4{\cdot}6H_2O$). pH on Enceladus simulation (Fig. 10) ranged from 5.74 to 6.76, and a_w ranged from 0.80 to 0.82, which are relatively favorable for life as we know it.

(4) A subsurface "ocean" on Titan was simulated with NH_4^+, Cl^-, SO_4^{2-}, $CH_4(g)$, and $NH_3(aq)$ over the temperature range of 173–273 K that led to precipitation of $(NH_4)_2SO_4$, ice, $CH_4{\cdot}6H_2O$, and NH_4Cl. pH on Titan simulation (Fig. 11) ranged from 11.24 to 18.03 (latter may not be accurate), and a_w ranged from 0.28 to 0.72, which are relatively unfavorable for life as we know it.

(5) On the Titan simulations, total pressures of 10, 250, and 1000 bars led to similar depositions, except for ice that failed to form under 1000 bars of pressure.

(6) In the past, there have been arguments for why Titan, given an early environment similar to Earth, could be a highly favorable body in our Solar System for life. But if Titan oceans are highly alkaline (high pH), then Enceladus that was lower alkaline (moderate pH) would seem a better environment for life as we know it on Earth.

(7) A popular model for the origin of life on Earth, involving lightning-induced chemistry acting on a CO_2–NH_3-rich atmosphere (Raulin and Toupance, 1977), might be invalidated by the high aqueous reactivity of these molecules expected in the Earth's interior. A modification of that model for biogenesis might simply move the prebiotic chemistry underground, where reactivity is promoted by hydrothermal conditions and production of free radicals; then ammonium thiocyanate, other ammonium salts, and other prebiotic and biologically important molecules could then be removed

from the crust by erosion and transported to the sea, where biogenesis might have taken place.

(8) Caution must be exercised in quantifying the ammonia/ammonium salt cases because of the complexities and limitations of these chemistries in the FREZCHEM model.

Finally, to address the issues of relevance raised in the preceding section, if ammonium silicates and ammonium salts are comparatively rare on Earth, they seem to be even rarer in meteorites. Gradually, evidence has accumulated that ammonium and ammonia do exist in some meteorites and on some outer planet satellite and Kuiper Belt Objects, as well as in vapor emissions from comets and Enceladus. However, the case for ammonium silicates in particular seems as close to a null set as possible; and the question then is why, if other ammonium compounds and ammonia exist, even if sparsely. Conversely, if pH is widely buffering compositions mainly in the ammonia (rather than ammonium) stability field, why do not we see more ammonia? Of course with ammonia in meteorites on Earth, volatility is an issue; and with ammonia and ammonium minerals on planetary surfaces, difficulties of detection and issues of stability against photolysis have been long-standing concerns. Perhaps the best evidence for ammonia is from the vapor detection in gases venting from comets and from Enceladus. In these cases, carbon dioxide greatly exceeds the amount of ammonia. Considering the high cosmic abundance of nitrogen, then the low abundance of ammonia being vented is explicable either by the nitrogen being mainly in the form of molecular nitrogen or by ammonia being sequestered as ammonium compounds in places where we mainly do not see them: not on the surfaces, but in the relatively warm interiors of icy moons and Kuiper Belt Objects.

Acknowledgments

Funding was provided by a NASA Outer Planets Research Project, "Modeling Complex Geochemical Processes in the Outer Planet Regions" and for J.I.L. from the NASA Astrobiology Institute. We thank Lisa Wable for help in preparing this manuscript.

References

Airieau, S.A., Farquhar, J., Thiemens, M.H., Leshin, L.A., Bao, H., Young, E., 2005. Planetesimal sulfate and aqueous alteration in CM and CI carbonaceous chondrites. Geochim. Cosmochim. Acta 69, 4166–4171.

Andersen, T.E., Burke, A.J., Neumann, E.R., 1995. Nitrogen-rich fluid in the upper mantle: Fluid inclusions in spinel dunite from Lanzarote, Canary Islands. Contrib. Mineral. Petrol. 120 (1), 20–28.

Atreya, S.K. et al., 2006. Titan's methane cycle. Plant. Space Sci. 54, 1177–1187.

Baker, V.R. et al., 2005. Extraterrestrial hydrogeology. Hydrogeol. J. 13, 51–68.

Barker, D.S., 1964. Ammonium in alkali feldspars. Am. Mineral. 49, 851–854.

Beghin, C., Sotin, C., Hamelin, M., 2010. Titan's native ocean revealed beneath some 45 km of ice by a Schumann-like resonance. C. R. Geosci. 342, 425–433.

Bos, A., Duit, W., van der Eerdem, A.M.J., Jansen, J.B., 1988. Nitrogen storage ion biotite: An experimental study of the ammonium and potassium partitioning between lM-phlogopite and vapor at 2 kb. Geochim. Cosmochim. Acta 52, 1275–1283.

Bostrom, K., Fredriksson, K., 1964. Surface conditions of the Orgueil Meteorite parent body as indicated by mineral associations. Smithsonian Misc. Coll. 151.

Bottrell, S.H., Miller, M.F., 1990. The geochemical behaviour of nitrogen compounds during the formation of black shale hosted quartz-vein gold deposits, north Wales. Appl. Geochem. 5, 289–296.

Brown, M.E., Calvin, W.M., 2000. Evidence for crystalline water and ammonia ices on Pluto's satellite Charon. Science 287, 107–109.

Brown, R.H. et al., 2006. Composition and physical properties of Enceladus' surface. Science 311, 1425–1428.

Burgess, R., Wright, I.P., Pillinger, P.T., 1991. Determinations of sulphur-bearing components in C_1 and C_2 carbonaceous chondrites by stepped combustion. Meteorities 26, 55–64.

Callahan, M.P. et al., 2011. Carbonaceous meteorites contain a wide range of extraterrestrial nucleobases. Proc. Nat. Acad. Sci. <http://www.pnas.org/cgi/doi/10.1073/pnas.1106493108>.

Clegg, S.L., Brimblecombe, P., 1989. Solubility of ammonia in pure aqueous and multicomponent solutions. J. Phys. Chem. 93, 7237–7248.

Clegg, S.L., Brimblecombe, P., 1995. Application of a multicomponent thermodynamic model to activities and thermal properties of 0–40 mol kg^{-1} aqueous sulfuric acid from <200 to 328 K. J. Chem. Eng. Data. 40, 43–64.

Cook, J.C., Desch, S.J., Roush, T.L., Trujillo, C.A., Geballe, T.R., 2007. Near-infrared spectroscopy of Charon: Possible evidence for cryovolcanism on Kuiper Belt Objects. Astrophys. J. 663, 1406–1419.

Cooper, J.F., Cooper, P.D., Sittler, E.C., Sturner, S.J., Rymer, A.M., 2009. Old Faithful model for radiolytic gas-driven cryovolcanism at Enceladus. Plant. Space Sci. 57, 1607–1620.

Coustenis, A., 2007. What Cassini–Huygens has revealed about Titan. Astron. Geophys. 48, 14–20.

Croft, S.K., Lunine, J.I., Kargel, J.S., 1988. Equation of state of ammonia–water liquid: Derivation and planetological application. Icarus 73, 279–293.

Cruikshank, D.P. et al., 2005. A spectroscopic study of the surfaces of Saturn's large satellites: H_2O ice, tholins, and minor constituents. Icarus 175, 268–283.

Dreibus, G., Wanke, H., 1987. Volatiles on Earth and Mars: A comparison∗. Icarus 71, 225–240.

Duit, W., Jansen, J.B.H., van Breemen, A., Bos, A., 1986. Ammonium micas in metamorphic rocks as exemplified by Dome de L'Agout (France). Am. J. Sci. 286, 702–732.

Erd, R.C., White, D.E., Fahey, J.J., Lee, D.E., 1964. Buddingtonite, an ammonium feldspar with zeolitic water. J. Mineral. Soc. Am. 49, 831–850.

Eugster, H.P., Munoz, J., 1966. Ammonium micas: Possible sources of atmospheric ammonia and nitrogen. Science 151, 683–686.

Fortes, A.D., 2000. Exobiological implications of a possible ammonia–water ocean inside Titan. Icarus 146, 444–452.

Fortes, A.D., 2007. Metasomatic clathrate xenoliths as a possible source for the south polar plumes of Enceladus. Icarus 191, 743–748.

Fortes, A.D., 2012. Titan's internal structure and the evolutionary consequences. Plant. Space Sci. 60, 10–17.

Fortes, A.D., Grindrod, P.M., Trickett, S.K., Vocadlo, L., 2007. Ammonium sulfate on Titan: possible origin and role in cryovolcanism. Icarus 188, 139–153.

Fredriksson, K., Kerridge, J.F., 1988. Carbonates and sulfates in CI chondrites: Formation by aqueous activity on the parent body. Meteoritics 23, 35–44.

Gounelle, M., Zolensky, M.E., 2001. A terrestrial origin for sulfate veins in CI1 chondrites. Meteorit. Planet. Sci. 36, 1321–1329.

Grant, W.D., 2004. Life at low water activity. Philos. Trans. Roy. Soc. Lond. Ser. B – Biol. Sci. 359, 1249–1266.

Grindrod, P.M., Fortes, A.D., Nimmo, F., Feltham, D.L., Brodholt, J.P., Vocadlo, L., 2008. The long-term stability of a possible aqueous ammonium sulfate ocean inside Titan. Icarus 197, 137–151.

Hogenboom, D.L., Kargel, J.S., Consolmagno, G.J., Holden, T.C., Lee, L., Buyyounouski, M., 1997. The ammonia–water system and the chemical differentiation of icy satellites. Icarus 128, 171–180.

Hussmann, H., Sohl, F., Spohn, T., 2006. Subsurface oceans and deep interiors of medium-sized outer planet satellites and large trans-neptunian objects. Icarus 185, 258–273.

Jewitt, D.C., Luu, J., 2004. Crystalline water ice on the Kuiper Belt Object (50,000) Quaoar. Nature 432, 731–733.

Juster, T.C., Brown, P.E., Bailey, S.W., 1987. NH_3-bearing illite in very low-grade metamorphic rocks associated with coal, northeastern Pennsylvania. Am. Mineral. 72, 555–565.

Kargel, J.S., 1991. Brine volcanism and the interior structures of asteroids and icy satellites. Icarus 94, 368–390.

Kargel, J.S., 1992. Ammonia–water volcanism on icy satellites: Phase relations at 1 atmosphere. Icarus 100, 556–574.

Kargel, J.S., 1998. The salt of Europa. Science 280, 1211–1212.

Kargel, J.S., Croft, S.K., Lunine, J.I., Lewis, J.S., 1991. Rheological properties of ammonia–water liquids and crystal-liquid slurries: Planetological applications. Icarus 89, 93–112.

Kargel, J.S. et al., 2000. Europa's salty crust and ocean: origin, composition, and prospects for life. Icarus 148, 226–265.

Kieffer, S.W., Jakosky, B.M., 2008. Enceladus—Oasis or ice ball? Science 320, 1432–1433.

Kieffer, S.W., Lu, X., Bethke, C.M., Spencer, J.R., Marshak, S., Navrotsky, A., 2006. A clathrate reservoir hypothesis for Enceladus' south polar plume. Science 314, 1764–1766.

King, T.V.V., Clark, R.N., Calvin, W.M., Sherman, D.M., Swayze, G.A., Brown, R.H., 1991. Evidence for ammonium-bearing minerals on Ceres. Lunar Planet. Sci. XXII, 717–718 (abstract).

Krohn, M.D., Kendall, C., Evans, J.R., Fries, T.L., 1993. Relations of ammonium minerals at several hydrothermal systems in the western US. J. Volcanol. Geotherm. Res. 56, 401–413.

Krumgalz, B.S., Pogorelsky, R., Pitzer, K.S., 1996. Volumetric properties of single aqueous electrolytes from zero to saturation concentration at 298.15 K represented by Pitzer's ion-interaction equations. J. Phys. Chem. Ref. Data 25, 663–689.

Leliwa-Kopystynski, J., Maruyama, M., Nakajima, T., 2002. The water–ammonia phase diagram up to 300 MPa: Application to icy satellites. Icarus 159, 518–528.

Levinson, A.A., Day, J.J., 1968. Low temperature hydrothermal synthesis of montmorillonite, ammonium-micas, and ammonium zeolites. Earth Planet. Sci. Lett. 5, 52–54.

Lewis, J.S., 1972. Low temperature condensation from the solar nebula. Icarus 16, 241–252.

Lide, D.R., 1994. CRC Handbook of Chemistry and Physics, 75th ed. CRC Press, Boca Raton.

Linke, W.F., 1965. Solubilities of Inorganic and Metal Organic Compounds, vol. II, fourth ed. Am. Chem. Soc, Washington, DC.

Lorenz, R.D., 2008. The changing face of Titan. Phys. Today 60, 34–39.

Lorenz, R.D. et al., 2008. Titan's rotation reveals an internal ocean and changing zonal winds. Science 318, 1649–1651.

Mahaffy, P.R., 2005. Intensive Titan exploration begins. Science 308, 969–970.

Manga, M., Wang, C.-Y., 2007. Pressurized oceans and the eruption of liquid water on Europa and Enceladus. Geophy. Res. Lett. 34, L07202. http://dx.doi.org/10.1029/2007GL029297.

Margulis, L., Halvorson, H.O., Lewis, J., Cameron, A.G.W., 1977. Limitations to growth of microorganisms on Uranus, Neptune, and Titan. Icarus 30, 793–808.

Marion, G.M., 2001. Carbonate mineral solubility at low temperatures in the Na–K–Mg–Ca–H–Cl–SO_4–OH–HCO_3–CO_3–CO_2–H_2O system. Geochim. Cosmochim. Acta 65, 1883–1896.

Marion, G.M., 2002. A molal-based model for strong acid chemistry at low temperatures (<200–298 K). Geochim. Cosmochim. Acta 66, 2499–2516.

Marion, G.M., Farren, R.E., 1999. Mineral solubilities in the Na–K–Mg–Ca–Cl–SO_4–H_2O system: A re-evaluation of the sulfate chemistry in the Spencer–Møller–Weare model. Geochim. Cosmochim. Acta 63, 1305–1318.

Marion, G.M., Kargel, J.S., 2008. Cold Aqueous Planetary Geochemistry with FREZCHEM: From Modeling to the Search for Life at the Limits. Springer, Berlin.

Marion, G.M., Catling, D.C., Kargel, J.S., 2003. Modeling aqueous ferrous iron chemistry at low temperatures with application to Mars. Geochim. Cosmochim. Acta 67, 4251–4266.

Marion, G.M., Kargel, J.S., Catling, D.C., Jakubowski, S.D., 2005. Effects of pressure on aqueous chemical equilibria at subzero temperatures with applications to Europa. Geochim. Cosmochim. Acta 69, 259–274.

Marion, G.M., Catling, D.C., Kargel, J.S., 2006. Modeling gas hydrate equilibria in electrolyte solutions. CALHAD 30, 248–259.

Marion, G.M., Kargel, J.S., Catling, D.C., 2008. Modeling ferrous-ferric iron chemistry with application to Martian surface geochemistry. Geochim. Cosmochim. Acta 72, 242–266.

Marion, G.M., Catling, D.C., Kargel, J.S., 2009a. Br/Cl portioning in chloride minerals in the Burns formation on Mars. Icarus 200, 436–445.

Marion, G.M. et al., 2009b. Modeling aluminum–silicon chemistries and application to Australian acidic playa lakes as analogues for Mars. Geochim. Cosmochim. Acta 73, 3493–3511.

Marion, G.M., Catling, D.C., Zahnle, K.J., Claire, M.W., 2010a. Modeling aqueous perchlorate chemistries with applications to Mars. Icarus 207, 675–685.

Marion, G.M., Mironenko, M.V., Roberts, M.W., 2010b. FREZCHEM: A geochemical model for cold aqueous solutions. Comput. Geosci. 36, 10–15.

Marion, G.M., Catling, D.C., Crowley, J.K., Kargel, J.S., 2011. Modeling hot spring chemistries with applications to martian silica formation. Icarus 212, 629–642.

Matson, D.L., Castillo, J.C., Lunine, J., Johnson, T.V., 2007. Enceladus' plume: Compositional evidence for a hot interior. Icarus 187, 569–573.

McKinnon, W.B., Zolensky, M.E., 2003. Sulfate content of Europa's ocean and shell: Evolutionary considerations and geological and astrobiological implications. Astrobiology 3, 879–897.

McKinnon, W.B., Prialnik, D., Stern, S.A., Coradini, A., 2008. Structure and evolution of Kuiper Belt Objects and Dwarf planets. In: Barucci, M.A., Boehnhardt, H., Cruikshank, D.P., Morbidelli, A. (Eds.), The Solar System Beyond Neptune. Univ. Arizona Press, Tucson, pp. 213–241.

Millero, F.J., 2001. The Physical Chemistry of Natural Waters. Wiley Intersci., New York.

Mitri, G., Showman, A.P., Lunine, J.I., Lorenz, R.D., 2007. Hydrocarbon lakes on Titan. Icarus 186, 385–394.

Mousis, O., Gautier, D., Bockelee-Morvan, D., 2002. An evolutionary turbulent model of Saturn's subnebula: Implications for the origin of the atmosphere of Titan. Icarus 156, 162–175.

Nimmo, F., Spencer, J.R., Pappalardo, R.T., Mullen, M.E., 2007. Shear heating as the origin of the plumes and heat flux on Enceladus. Nature 447, 289–291.

Norman, L.H., Fortes, A.D., 2011. Is there life on...Titan? Astrobiol. 52, 1.39–1.42.

Osegovic, J.P., Max, M.D., 2005. Compound clathrate hydrate on Titan's surface. J. Geophys. Res. 110, E08004. http://dx.doi.org/10.1029/2005JE002435.

Parkinson, C.D. et al., 2007. Enceladus: Cassini observations and implications for the search for life (Research Note). Astron. Astrophys. 463, 353–357.

Pitzer, K.S., 1991. Ion interaction approach: Theory and data correlation. In: Pitzer, K.S. (Ed.), Activity Coefficients in Electrolyte Solutions, second ed. CRC Press, Boca Raton, pp. 75–153.

Pitzer, K.S., 1995. Thermodynamics, third ed. McGraw-Hill, New York.

Pizzarello, S., Feng, X., Epstein, S., Cronin, J.R., 1994. Isotopic analysis of nitrogenous compounds from the Murchison meteorite: Ammonia, amines, amino acids, and polar hydrocarbons. Geochim. Cosmochim. Acta 58, 5579–5587.

Pizzarello, S., Williams, L.B., Lehman, J., Holland, G.P., Yarger, J.L., 2011. Abundant ammonia in primitive asteroids and the case for a possible exobiology. Proc. Natl. Acad. Sci. 108, 4303–4306.

Porco, C.C. et al., 2006. Cassini observes the active south pole of Enceladus. Science 311, 1393–1401.

Postberg, F. et al., 2009. Sodium salts in E-ring ice grains from an ocean below the surface of Enceladus. Nature 459, 1098–1101.

Postberg, F., Schmidt, J., Hillier, J., Kempt, S., Srama, R., 2011. A salt-water reservoir as the source of compositionally stratified plume on Enceladus. Nature 474, 620–622.

Que, H., Chen, C.-C., 2011. Thermodynamic modeling of the NH_3–CO_2–H_2O system with electrolyte NRTL model. Ind. Eng. Chem. Res. 50, 11406–11421.

Raulin, F., Toupance, G., 1977. Role of sulfur in chemical evolution. J. Mol. Evol. 9, 329–338.

Rivkin A.S., 1997. Observations of Main-Belt Asteroids in the 3-μm Region. Ph.D. Dissertation, University of Arizona, Tucson.

Rivkin, A.S., Volquardsen, E.L., Clark, B.E., 2006. The surface composition of Ceres: Discovery of carbonates and iron-rich clays. Icarus 185, 563–567.

Robinson, R.A., Stokes, R.H., 1970. Electrolyte Solutions, second ed. (revised). Butterworths, London.

Rosenberg, N.D., Browning, L., Bourcier, W.L., 2001. Modeling aqueous alteration of CM carbonaceous chondrites. Meteorit. Planet. Sci. 36, 239–244.

Santana, H., Pelisson, L., Janiaski, D.R., Thaïs, C., Zaia, B.V., Zaia, D.A.M., 2010. UV radiation and the reaction between ammonium and thiocyanate under prebiotic chemistry conditions. J. Serb. Chem. Soc. 75, 1381–1389.

Schulze-Makuch, D., Grinspoon, D.H., 2005. Biologically enhanced energy and carbon cycling on Titan? Astrobiology 5, 560–567.

Smirnov, A., Hauser, D., Laffers, R., Strongin, D.R., Schoonen, M.A.A., 2008. Abiotic ammonium formation in the presence of Ni–Fe metals and alloys and its implications for the Hadean nitrogen cycle. Geochem. Trans. 9, 5. http://dx.doi.org/10.1186/1467-4866-9-5, http://www.geochemicaltransactions.com/content/9/1/5.

Smythe, W.D., Nelson, R., Boryta, M.D., 2009. Anhydrous ammonia frost on Titan. Eos Trans. AGU (Fall Suppl.) 90(52). Abstract P21B-1215.

Sohl, F. et al., 2010. Subsurface water oceans on icy satellites: Chemical composition and exchange processes. Space Sci. Rev. 153, 485–510.

Sotin, C., 2007. Titan's lost seas found. Nature 445, 29–30.

Sotin, C., Tobie, G., 2008. Titan's hidden ocean. Science 319, 1629–1630.

Spencer, J., Grinspoon, D., 2007. Inside Enceladus. Nature 445, 376–377.

Spencer, J.R. et al., 2006. Cassini encounters Enceladus: Background and the discovery of a south polar hot spot. Science 311, 1401–1405.

Stofan, E.R. et al., 2007. The lakes of Titan. Nature 445, 61–64.

Swanson, B.D., 2009. How well does water activity determine homogeneous ice nucleation temperature in aqueous sulfuric acid and ammonium sulfate droplets? J. Atmos. Sci. 66, 741–754.

Tobie, G., Grasset, O., Lunine, J.I., Mocquet, A., Sotin, C., 2005. Titan's internal structure inferred from a coupled thermal–orbital model. Icarus 175, 496–502.

Tokano, T. et al., 2006. Methane drizzle on Titan. Nature 442, 432–435.

Vedder, W., 1965. Ammonium in muscovite. Geochim. Cosmochim. Acta 29, 221–228.

Voncken, J.H.L., van Roermundt, H.L.M., van der Eerden, A.M.J., Jansen, J.B.H., Erd, R.C., 1993. Holotype buddingtonite: An ammonium feldspar without zeolitic H_2O. Am. Mineral. 78, 204–209.

Waite Jr., J.H. et al., 2006. Cassini ion and neutral mass spectrometer: Enceladus plume composition and structure. Science 311, 1419–1422.

Waite Jr., J.H. et al., 2009. Liquid water on Enceladus from observations of ammonia and ^{40}Ar in the plume. Nature 460, 487–490.

Waite, J.H. et al., 2011. Enceladus' plume composition. EPSC-DPS Joint Meeting. Abstract 61-4.

Watenphul, A., Wunder, B., Wirth, R., Heinrich, W., 2010. Ammonium-bearing clinopyroxene: A potential nitrogen reservoir in the Earth's mantle. Chem. Geol. 270, 240–248.

Wu, J., Huang, Z., Luo, T., 2004. Contents of fixed-ammonium (NH_4^+) in lamprophyres in the Zhenyuan gold orefield, Yunnan Province, China: Implications for its characteristics of the source region. Chin. J. Geochem. 23 (2), 186–190.

Yokano, T. et al., 2006. Methane drizzle on Titan. Nature 442, 432–435.

Young, E., 2000. Charon's first detailed spectra hold many surprises. Science 287, 53–54.

Zolensky, M.E., Bourcier, W.L., Gooding, J.L., 1989. Aqueous alteration on the hydrous asteroids—Results of computer simulations. Icarus 78, 411–425.

Zolensky, M., Barrett, R., Browning, L., 1993. Mineralogy and composition of matrix and chondrule rims in carbonaceous chondrite. Geochim. Cosmochim. Acta 57, 3123–3148.

Zolensky, M.E. et al., 1997. CM chondrites exhibit the complete petrologic range from type 2 to 1. Geochim. Cosmochim. Acta 61, 5099–5115.

Zolotov, M.Yu., 2007. An oceanic composition on early and today's Enceladus. Geophy. Res. Lett. 34, L23203. http://dx.doi.org/10.1029/2007GL031234.

Zolotov, M.Yu., 2009. On the composition and evolution of Ceres. Icarus 204, 183–193.

Zolotov, M.Yu., Kargel, J.S., 2009. On the composition of Europa's icy shell, ocean and underlying rocks. In: Pappalardo, R., McKinnon, W.B., Khurana, K. (Eds.), Europa. Univ. Ariz. Press, Tucson, pp. 431–457.

Zolotov, M.Yu., Shock, E.L., 2001. A hydrothermal origin for the sulfate-rich ocean of Europa. Lunar and Planet. Sci. XXXII. Abstract 1990 [CD-ROM].

Zolotov, M.Yu., Tobie, G., Postberg, F., Magee, B., Waite, J.H., Esposito, L., 2011. Chemical and phase composition of Enceladus: Insights from Cassini data. EPSC-DPS Joint Meeting. Abstract 1330.